CDF/ANAL/BOTTOM/CDFR/10213
Version 1.0
August 2, 2010

Measurement of Time-integrated CP Violating Asymmetry in $D^0 \to \pi^+\pi^-$ Decays

A. Di Canto[1,2], M. J. Morello[3], G. Punzi[1,3], L. Ristori[2], and D. Tonelli[3]
[1]University of Pisa; [2]INFN Pisa; [3]Fermilab

Abstract

This note describes a novel, fully data-driven, measurement of the CP violating asymmetry in $D^0 \to \pi^+\pi^-$ decays using about 5.94 fb^{-1} of CDF data. We use the strong $D^{\star+} \to D^0\pi^+$ decay ("$D^\star$ tag") to identify the flavor of the charmed meson at production time and exploit CP-conserving strong $c\bar{c}$ pair-production in $p\bar{p}$ collisions. Higher statistic samples of Cabibbo-favored $D^0 \to K^-\pi^+$ decays with and without $D^\star$ tag are used to highly suppress systematic uncertainties due to detector effects. The result, $A_{\rm CP}(\pi\pi) = \big[0.22 \pm 0.24\ (stat.) \pm 0.10\ (syst.)\big]\%$, is the world's most precise measurement to date and it is fully consistent with no CP violation.

1 Introduction and motivation

The rich phenomenology of neutral flavored mesons provides many experimentally accessible observables sensitive to virtual contributions of non-Standard Model (SM) particles or couplings. Presence of non-SM physics may alter the expected decay rates, or flavor-mixing rates, or introduce additional sources of CP-violation besides the CKM phase. The physics of neutral kaons and bottom mesons has been extensively explored in dedicated experiments using kaon beams or e^+e^- collisions at the $\Upsilon(4S)$ resonance. The physics of bottom-strange mesons is currently being studied in detail by the CDF and D0 experiments. In spite of the success of several dedicated experiments in the '80–'90, experimental sensitivities reached in the charm sector were still orders of magnitude far from the most optimistic of the SM and non-SM expectations. This, combined with significantly more uncertain predictions with respect to the B and K sectors, because of the intermediate value of the charm quark mass, too

light for factorization of hadronic amplitudes and too heavy for applying chiral symmetry, made the experimental advancement in the charm sector slower. However, studies of CP violation in charm meson decays provides a unique probe of new physics. The SM predicts effects smaller than $\mathcal{O}(10^{-3})$ [1], as expected in charm sector transitions, which involve only the first two quark families, whose CKM phases are suppressed. Any significant deviation at the present level of experimental sensitivities would clearly signal non-SM contributions. More importantly, the neutral D system is the only one where the external up-sector quarks are involved. Thus it probes scenarios where the up sector plays a special role, such as supersymmetric models with alignment and, more generally, models in which CKM mixing is generated in the up sector. Finally, singly Cabibbo-suppressed decays are sensitive to new physics contributions to penguin and dipole operators.

CDF has today the world's largest samples of exclusive charm meson decays in charged final states, with signal purities competitive with those of the B-factories. This is an unexpected but welcome by-product of the success of the trigger on displaced tracks. Large samples of charm decays can be used to measure CP violating asymmetries and charm mixing phenomenology with unprecedented sensitivity, probing for the first time significant portions of the space of non-SM physics parameters.

Time integrated CP-violating asymmetries of singly-Cabibbo transitions as $D^0 \to \pi^+\pi^-$ and $D^0 \to K^+K^-$ are powerful probes of non-SM physics. The contribution to these decays from "penguin" amplitudes are in SM negligible [1], but that is the place, together with $D^0 - \overline{D}^0$ oscillations, where non-SM particles could play a role enhancing the size of CP-violation with respect to the SM expectation. Any significant asymmetry above the $\mathcal{O}(0.1\%)$ level expected in the CKM hierarchy would unambiguously indicate non-SM physics.

We present a measurement of time-integrated CP violating asymmetry in the Cabibbo-suppressed $D^0 \to \pi^+\pi^-$ decay:

$$A_{\rm CP}(\pi^+\pi^-) = \frac{\Gamma(D^0 \to \pi^+\pi^-) - \Gamma(\overline{D}^0 \to \pi^-\pi^+)}{\Gamma(D^0 \to \pi^+\pi^-) + \Gamma(\overline{D}^0 \to \pi^-\pi^+)}, \tag{1}$$

This quantity could receive contribution from different amplitudes in D^0 and $\overline{D}^0$ decays (direct CP violation) but also from mixing induced effects (indirect CP violation). In particular the latter source produces a time-dependent asymmetry, which expression when neutral charmed mesons decay into CP eigenstates is [1]

$$A_{\rm CP}(t) \approx \eta_{CP} \left[\frac{y}{2} \frac{t}{\tau} \left(\left|\frac{p}{q}\right| - \left|\frac{q}{p}\right| \right) \cos\varphi + \sin\left(x \frac{t}{\tau} \right) \sin\varphi \right], \tag{2}$$

that persists when integrated over time. In eq. (2) η_{CP} is the CP-parity of the decay final state ($+1$ for $\pi^+\pi^-$), x, y, p and q are the usual parameters used to describe flavored mesons mixing, φ is the weak CP violating phase and t/τ the proper decay time in unit of D^0 lifetime

Experiment	$A_{CP}(\pi^+\pi^-)$ (%)
Babar on 386/fb	-0.24 ± 0.52 (*stat.*) ± 0.22 (*syst.*)
Belle on 540/fb	-0.43 ± 0.52 (*stat.*) ± 0.12 (*syst.*)
CDF on 123/pb	$+1.0 \pm 1.3$ (*stat.*) ± 0.6 (*syst.*)

Table 1: Current best measurements [2] and published CDF result [3].

($\tau \approx 0.5$ ps). The measured integrated asymmetry, owing to the slow mixing rate of charm mesons, is then at first order the sum of two terms:

$$A_{CP}(\pi^+\pi^-) = a_{CP}^{dir} + \int_0^\infty A_{CP}(t)\mathrm{D}(t)dt \approx a_{CP}^{dir} + \frac{\langle t \rangle}{\tau} a_{CP}^{ind}. \quad (3)$$

The first term arises from direct and the second one from indirect CP violation. The integration in eq. (3) is performed over the observed ditribution of proper decay time, $D(t)$. Since the value of $\langle t \rangle$ depends strongly on $D(t)$, different experimental configurations could measure different values of A_{CP} and this could result in different sensitivities to a_{CP}^{dir} or a_{CP}^{ind}. As an example, since the trigger that collected the data used in this analysis has requirements on the minimum impact parameter of the D^0 tracks, our samples will be enriched of high proper decay time candidates thus our measurement will be more sensitive to indirect instead of direct CP violation in $D^0 \to \pi^+\pi^-$ decays.

We first reconstruct a signal consistent with a $\pi^+\pi^-$ decay of a neutral charmed meson (D^0 or $\overline{D}^0$). Then we associate a low-momentum charged particle to the meson candidate to construct a $D^{\star+}$ (or $D^{\star-}$) candidate. The flavor of the charmed meson is unambiguously determined from the charge of the pion in the strong $D^{\star+} \to D^0\pi^+$ (or $D^{\star-} \to \overline{D}^0\pi^-$) decay. Knowing that primary D^0 and $\overline{D}^0$ mesons are produced in equal number in strong $p\bar{p}$ interactions, any asymmetry between the number of D^0 and $\overline{D}^0$ decays is due to either CP non-conservation or detector-induced reconstruction asymmetries. The physics asymmetry is extracted by subtracting the instrumental effects through a combination of charge-asymmetries measured in similar decays, as detailed in the next section. Charge conjugate states are implied unless otherwise stated.

Current experimental measurements of $A_{CP}(\pi\pi)$ are summarized in tab. 1. The published CDF result dates 2005 and has been obtained on the first 123 pb^{-1} of collected data, using a different analysis approach that was based on simulation to determine detector charge-asymmetries. Today CDF has the world's largest sample of charm decays and can provide a precise measurement of $A_{CP}(\pi\pi)$. Fig. 1 (a) shows the number, N, of tagged $D^0 \to \pi\pi$ candidates that pass our selection criteria (see details later) as a function of the integrated luminosity, with a good approximation the statistical resolution on $A_{CP}(\pi\pi)$ is simply $1/\sqrt{N}$ so as shown in fig. 1 (b) with the current sample of about 200×10^3 events we expect to have a measurement with a statistical uncertainty of about 0.22% that is two times better than

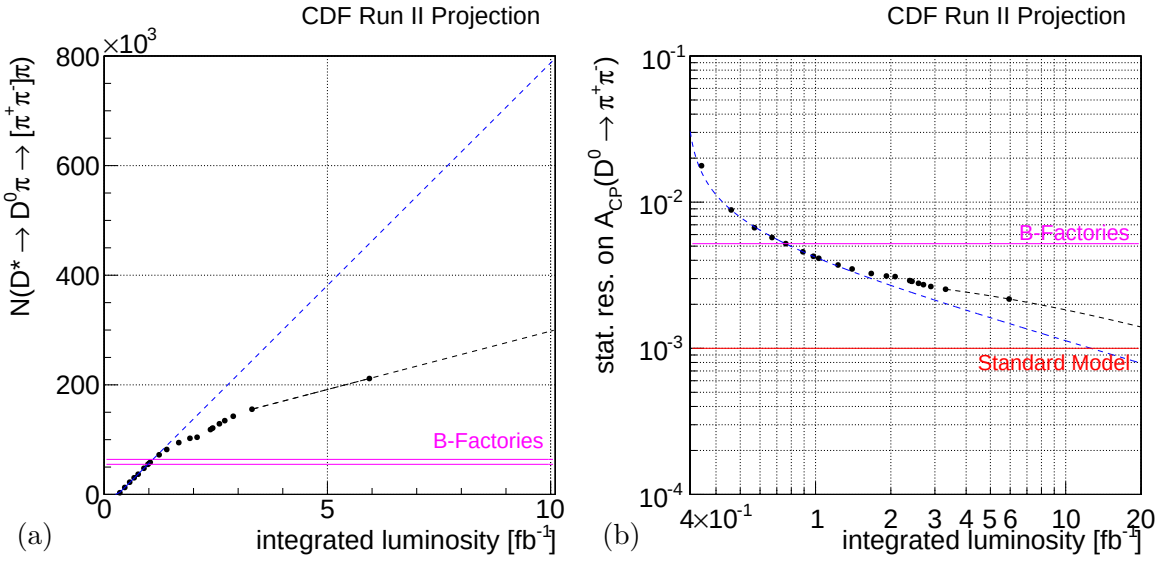

Figure 1: Number of tagged $D^0 \to \pi^+\pi^-$ candidates that pass our selection (a) and estimated statistical uncertainty on the asymmetry measurement (b) as a function of the collected integrated luminosity. The magenta lines indicate B-factories values [2] while the red line is an approximate upper limit from SM predictions. The blue (black) dashed line is the projection assuming a constant collection rate as it was in the early (latter) periods of data-taking.

current B-factories results.

The main challenge is that the COT layout is intrinsically charge asymmetric thus different detection efficiencies for positive and negative low-momentum tracks (soft pions, in our case) induce an instrumental asymmetry in the number of reconstructed $D^\star$–tagged D^0s and $\overline{D}^0$s. Other possible asymmetries may originate in slightly different performance between positive and negative tracks in pattern-reconstruction and track-fitting algorithms. The combined effect of these is a net asymmetry in the range of a few percents, as shown in fig. 2. This must be corrected to better than one permille to match the expected statistical precision of the present measurement.

We propose a novel, fully data-driven method that uses higher statistic samples of tagged and untagged Cabibbo-favored $D^0 \to K^-\pi^+$ decays to correct for all detector effects and aims at suppressing systematic uncertainties to below the statistical ones.

2 A method to suppress detector induced charge asymmetries

The procedure used to cancel detector induced asymmetries is briefly outlined here, while a detailed mathematical treatment in given in [4].

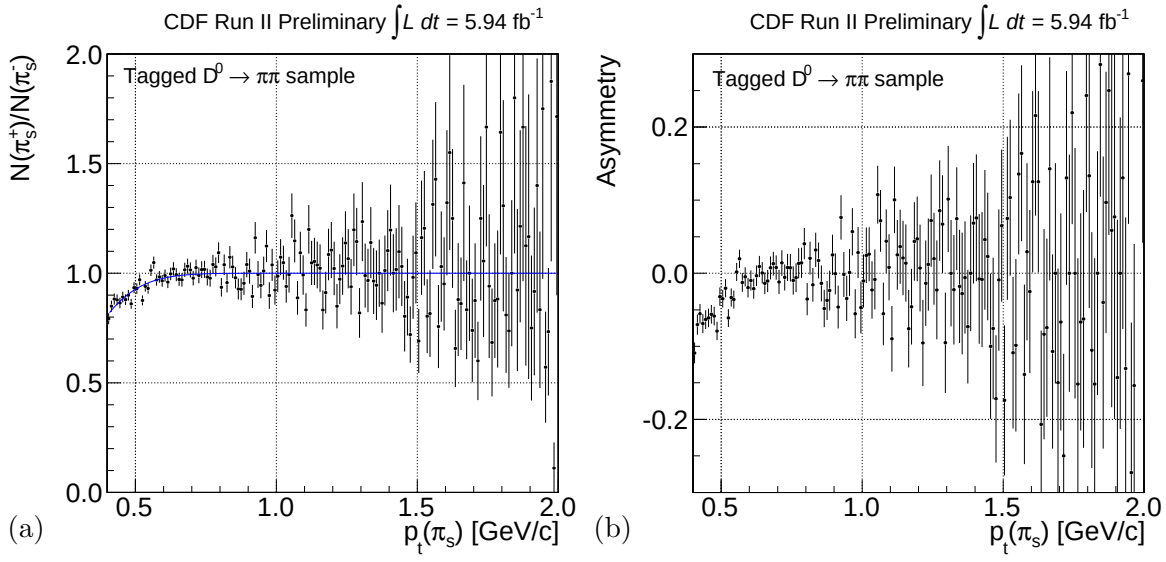

Figure 2: Soft pion charge ratio (a) and asymmetry (b) as a function of transverse momentum for a clean sample of $D^\star \to D^0\pi_s$ candidates with $D^0 \to \pi\pi$. The blue curve is the function in eq. (7).

What is directly measurable is the observed "raw" asymmetry,

$$A_{\rm CP}^{\rm raw}(D^0) = \frac{N_{\rm obs}(D^0) - N_{\rm obs}(\overline{D}^0)}{N_{\rm obs}(D^0) + N_{\rm obs}(\overline{D}^0)},$$

that is a composition of the physical CP violating asymmetry, the one expressed in eq. (1), and any kind of detector effect that induces an artificial asymmetry (indicated with δ from now on). We propose an appropriate combination of the values of the observed asymmetries of three different event samples,

1. $D^\star$-tagged $D^0 \to \pi^+\pi^-$ decays (or simply $\pi\pi^\star$)
2. $D^\star$-tagged $D^0 \to K^-\pi^+$ decays ($K\pi^\star$)
3. untagged $D^0 \to K^-\pi^+$ decays ($K\pi$)

to extract the value of $A_{\rm CP}(D^0 \to \pi^+\pi^-)$. The idea is that, neglecting terms of order $A_{\rm CP}\delta$ and δ^2, the observed asymmetries in the different samples are

$$\begin{aligned} A_{\rm CP}^{\rm raw}(\pi\pi^\star) &= A_{\rm CP}(\pi\pi) + \delta(\pi_s)^{\pi\pi^\star} \\ A_{\rm CP}^{\rm raw}(K\pi^\star) &= A_{\rm CP}(K\pi) + \delta(\pi_s)^{K\pi^\star} + \delta(K\pi)^{K\pi^\star} \\ A_{\rm CP}^{\rm raw}(K\pi) &= A_{\rm CP}(K\pi) + \delta(K\pi)^{K\pi}, \end{aligned} \tag{4}$$

where

- $\delta(\pi_s)^{\pi\pi^\star}$ is the instrumental asymmetry between reconstructing a positive or negative soft pion associated to a $\pi^+\pi^-$ charm decay. This is mainly induced by charge-asymmetric track-reconstruction efficiency at low transverse momentum.

- $\delta(\pi_s)^{K\pi^\star}$ is the instrumental asymmetry between reconstructing a positive or negative soft pion associated to a $K^+\pi^-$ or $K^-\pi^+$ charm decay. This is mainly induced by charge-asymmetric track-reconstruction efficiency at low transverse momentum.

- $\delta(K\pi)^{K\pi}$ and $\delta(K\pi)^{K\pi^\star}$ are the instrumental asymmetry between reconstructing a $K^+\pi^-$ or a $K^-\pi^+$ charm decay respectively for the untagged and the tagged case. These are mainly induced by the difference in interaction cross-section with matter between positive and negative kaons. Smaller effect are due to charge-curvature asymmetries in track triggering and reconstruction.

All the above effects can vary as a function of a number of kinematic variables or environmental conditions in the detector. If the kinematic distributions of soft pions are consistent in $K\pi^\star$ and $\pi\pi^\star$ samples, and if the distributions of D^0 decay products are consistent in $K\pi^\star$ and $K\pi$ samples, then $\delta(\pi_s)^{\pi\pi^\star} \approx \delta(\pi_s)^{K\pi^\star}$ and $\delta(K\pi)^{K\pi^\star} \approx \delta(K\pi)^{K\pi}$. The CP violating asymmetry then becomes accessible as

$$A_{\rm CP}(\pi\pi) = A_{\rm CP}^{\rm raw}(\pi\pi^\star) - A_{\rm CP}^{\rm raw}(K\pi^\star) + A_{\rm CP}^{\rm raw}(K\pi) \tag{5}$$

The cancellation provided by this formula relies on some basic assumptions:

- $p\bar{p}$ strong interactions are charge symmetric, i.e. primary D^0 and $\overline{D}^0$ mesons are produced in equal number and so primary $D^{\star+}$ and $D^{\star-}$ mesons;

- small charge asymmetries in D^0 and $\overline{D}^0$ production as a function of η could be caused by beam drag effects. This asymmetry is constrained to change sign for opposite η thus the net effect cancel out as long as the distribution of our decays are symmetric in η that is true at first order;

- the detection efficiency for the $D^\star$ can be expressed as the product of the efficiency for the soft pion times the efficiency for the D^0 final state.

Before applying this technique to real data we proved that our approach achieves the goal of suppressing detector induced asymmetries down to the permille level using Monte Carlo simulation (sec. 3). We apply the method to samples simulated with a wide range of physical and detector asymmetries to verify that the cancellation works regardless of the specific configuration. The Monte Carlo (MC) is used here only as an unbiased validation tool, but no MC input will enter the final results of the measurement.

3 Method validation

To be sensitive to permille effects we need MC samples with $\mathcal{O}(10^6)$ decays. And we need several of them to test a sufficiently broad set of different configurations for the input asymmetries. To achieve this goal in a realistic and reasonable time we decided to use a resampling technique applied to a smaller set of statistically independent simulated samples. We generated two B-MC samples (see sec. 3.1 for details): one of $D^{\star+} \to D^0\pi_s^+ \to [\pi^-\pi^+]\pi_s^+$ decays, used to reconstruct the tagged $\pi\pi$ sample, and another of $D^{\star+} \to D^0\pi_s^+ \to [K^-\pi^+]\pi_s^+$ decays, used to reconstruct either the tagged or the untagged $K\pi$ decays. For each of these three samples ('parent samples') we construct several resamplings (of equal or bigger size) by random sampling with replacement from the original dataset (bootstrapping). This provides several different high-statistics samples, nearly statistically independent, with features similar to the initial parent sample. Arbitrary input asymmetries are introduced and controlled by an event-specific weight applied to the "true" (GenP) information. The analysis applied to the reconstructed samples allows determination of observed asymmetries, $A_{\rm CP}^{\rm raw}(\pi\pi^\star)$, $A_{\rm CP}^{\rm raw}(K\pi^\star)$, $A_{\rm CP}^{\rm raw}(K\pi)$. Finally, applying eq. (5) we extract $A_{\rm CP}(\pi\pi)$ and verify that it is consistent with the input value.

A detailed description of the resampling/reweighting algorithm is given in sec. 3.2 while the results of different kind of tests we made are in sec. 3.3.

3.1 Monte Carlo samples

We use `BGenerator` to simulate the c-quarks production, using the standard charm spectrum available in the official B-MC release 6.1.4mc patch q, and their hadronization into $D^\star$ mesons and `EvtGen` to simulate the charmed mesons decays. Then the events are passed through the full CDF detector simulation (`cdfsim`, `TRGSim++`), production and finally ntuplized in the BStNtuple format [5] [6].

The detector and trigger configurations have undergone several variations during Run II. The simulation can access the database and thus allows simulation of the detailed configuration of any set of real data-taking runs for modeling the realistic detector response in any given subset of data. This feature is not relevant in our analysis, so to speed-up generation we generate just events mimicking the run configuration of periods 17–18.

3.2 Resampling/reweighting algorithm

The algorithm is based on a single event weight. For each event of the original parent B-MC sample we extract a non-negative integer "weight", w, that corresponds to the number of times the event will be repeated in the final resampled/reweighed dataset. The value of the weight depends on the chosen input values for the asymmetries, which can depend on the

features of the event itself.

The input quantities of the algorithm are:

- the resampling factor, N, a positive integer that correspond to the mean multiplication factor of the sample size;
- the reconstruction efficiency ratio of positive and negative pions, $\epsilon(\pi^+)/\epsilon(\pi^-)$, an arbitrary parameter used to mimic instrumental asymmetries due to pion reconstruction. This can be function of pion momenta, azimuthal angle, etc...;
- the reconstruction efficiency ratio of positive and negative kaons, $\epsilon(K^+)/\epsilon(K^-)$, analogous to above;
- the physical CP violating asymmetry $A_{\rm CP}(K\pi)$;
- the physical CP violating asymmetry $A_{\rm CP}(\pi\pi)$.

The algorithm for each event proceeds as follows. We extract from a Poisson distribution with mean N the number of repetitions n due to the resampling factor, so the value of w is initialized to n. For each of the n repetitions GenP information is used to keep or throw the repeated event according to the desired values of relative efficiencies and physical asymmetries. To apply a certain $r = \epsilon(\pi^+)/\epsilon(\pi^-)$ value, say less than one, we look for a positive pion in the GenP list, and for each pion found we extract from a uniform distributed probability a value p. If $p \geqslant r$ we decrease the current weight w of one unit.

The algorithm in details is the following:

1. Resampling: extract $n \sim \text{Poisson}(N)$ and initialize $w = n$.
2. Loop over $i \leqslant n$:
   - Reweight for a given efficiency ratio, there are two possible cases:
     (a) $\epsilon(\pi^+)/\epsilon(\pi^-) < 1$, so define $r_\epsilon = \epsilon(\pi^+)/\epsilon(\pi^-)$
       - look for all π^+ in the GenP list;
       - for each found extract $p \sim \text{Uniform}(0, 1)$, if none found continue;
       - if $p \geqslant r_\epsilon$ do $w - -$, otherwise continue;

     (b) $\epsilon(\pi^+)/\epsilon(\pi^-) > 1$, so define $r_\epsilon = \epsilon(\pi^-)/\epsilon(\pi^+)$
       - look for all π^- in the GenP list;
       - for each found extract $p \sim \text{Uniform}(0, 1)$, if none found continue;
       - if $p \geqslant r_\epsilon$ do $w - -$, otherwise continue;
   - Reweight for a given $A_{\rm CP}(\pi\pi)$ value, there are two possible cases:
     (a) $A_{\rm CP} > 0$, so define $r_{A_{\rm CP}} = N(\overline{D}^0)/N(D^0) = (1 + A_{\rm CP})/(1 - A_{\rm CP})$

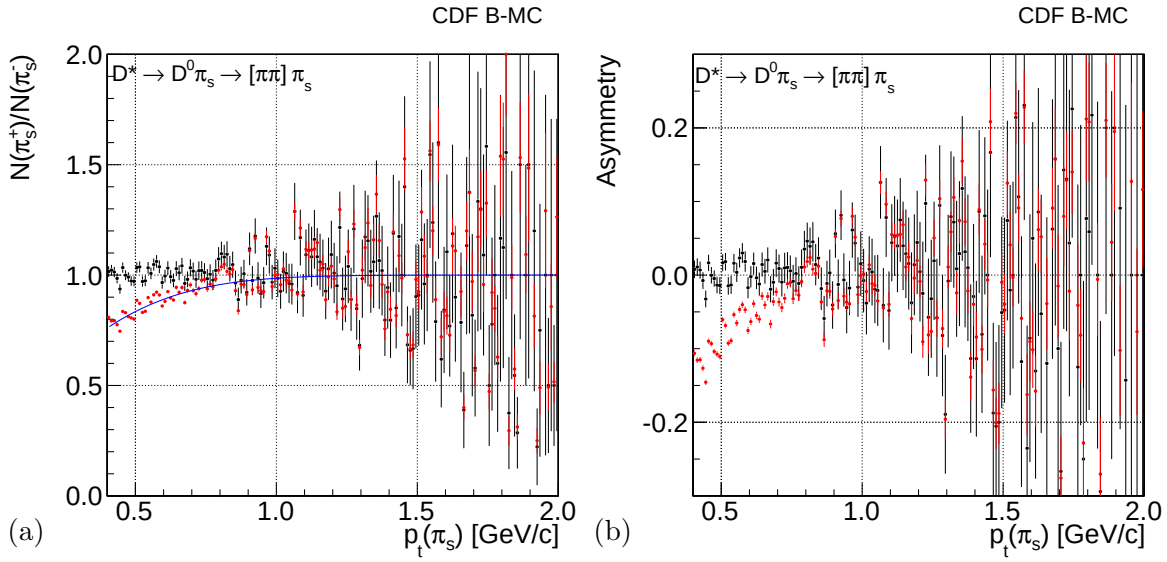

Figure 3: Soft pion charge ratio (a) and asymmetry (b) as a function of transverse momentum for the original B-MC sample of $D^\star \to D^0\pi_s \to [\pi^+\pi^-]\pi_s$ (black points) and for a resampled dataset (red points) of a factor 10 in which the efficiency ratio represented by the blue curve is introduced.

- look for a $\overline{D}^0 \to \pi^+\pi^-$ in the GenP list;
- if found extract $p \sim \text{Uniform}(0,1)$, otherwise continue;
- if $p \geqslant r_{A_{\rm CP}}$ do $w--$, otherwise continue;

(b) $A_{\rm CP} < 0$, so define $r_{A_{\rm CP}} = N(D^0)/N(\overline{D}^0) = (1 - A_{\rm CP})/(1 + A_{\rm CP})$

- look for a $D^0 \to \pi^+\pi^-$ in the GenP list;
- if found extract $p \sim \text{Uniform}(0,1)$, otherwise continue;
- if $p \geqslant r_{A_{\rm CP}}$ do $w--$, otherwise continue;

A similar procedure is used for the other two input variables $\epsilon(K^+)/\epsilon(K^-)$ and $A_{\rm CP}(K\pi)$. An unique algorithm is applied to all the three samples ($\pi\pi^\star$, $K\pi^\star$ and $K\pi$). Since we reconstruct also the untagged $D^0 \to K^-\pi^+$ decays from simulated $D^\star$ decays, in this case the pion coming from the $D^\star$ decay in the GenP list is not used to calculate the final weight.

Fig. 3 (a) shows, as an example, how the ratio of positive and negative soft pions as a function of the track transverse momentum changes after applying our algorithm: black points are the parent B-MC sample of $D^{\star+} \to D^0\pi_s^+ \to [\pi^+\pi^-]\pi_s^+$, in which the ratio is 1 in all the p_T range, while red points are a dataset resampled by a factor 10 after applying a reweight that uses as input the reconstruction efficiency ratio

$$\frac{\epsilon(\pi^+)}{\epsilon(\pi^-)} = \text{Erf}\left(\frac{3}{2}\, p_T + A\right) \tag{6}$$

with $A = 0.23$ and represented by the blue curve.

3.3 Validation results

We consider six different cases:

case 0 resampling $\times 10$;

case 1 resampling $\times 10$ and p_T-dependent $\epsilon(\pi^+/\pi^-)$ given by the expression in eq. (6);

case 2 resampling $\times 10$ and $\epsilon(K^+/K^-) = 98\%$ constant;

case 3 resampling $\times 10$ and $A_{\rm CP}(\pi\pi) = 1.1\%$;

case 4 resampling $\times 10$ and $A_{\rm CP}(K\pi) = 0.8\%$;

case 5 all of the above.

We reweight the three samples according to each of these cases and for each we measure the observed asymmetries. Then, using eq. (5) we compare the result with the known input $A_{\rm CP}(\pi\pi)$ value. Notice that owing to the finite size of the parent sample, small asymmetries due to statistical fluctuations are present there. Since we resample from this parent sample, these small asymmetries will remain in our resamplings and won't be cancelled by our procedure. The result obtained in each cases defined above will be subtracted by the $A_{\rm CP}(\pi\pi)$ value of the parent dataset. Tab. 2 reports, as an example, the results from a single test for the original dataset (the unweighted case) and the six different reweighting cases. In the last columns there are three different $A_{\rm CP}(\pi\pi)$ values: the absolute one is obtained using eq. (5) while the second is the $A_{\rm CP}(\pi\pi)$ value after subtracting the one obtained on the original unweighted sample, this is the one that should be compared with the input $A_{\rm CP}(\pi\pi)$ value.

The resulting $A_{\rm CP}(\pi\pi)$ from a single test is always in good agreement with the expectation from the parent sample. This test was repeated 100 times. Fig. 4 shows the distributions of the bias,

$$\Delta A_{\rm CP} = A_{\rm CP} - A_{\rm CP}(\text{unweighted}) - A_{\rm CP}(\text{input}),$$

case by case; the distributions have mean value compatible with zero and RMS of about 0.08% as expected.

Reweighting case	$A_{\rm CP}^{\rm raw}(\pi\pi^\star)$ (%)	$A_{\rm CP}^{\rm raw}(K\pi^\star)$ (%)	$A_{\rm CP}^{\rm raw}(K\pi)$ (%)	$A_{\rm CP}(\pi\pi)$ (%)		
				absolute	wrt unw. case	input value
Unweighted	-0.32 ± 0.15	$+0.37 \pm 0.16$	$+0.34 \pm 0.15$	-0.36 ± 0.27	-	-
0	-0.36 ± 0.05	$+0.38 \pm 0.05$	$+0.32 \pm 0.05$	-0.41 ± 0.08	-0.05 ± 0.08	0.00
1	$+4.22 \pm 0.05$	$+4.91 \pm 0.05$	$+0.32 \pm 0.05$	-0.37 ± 0.09	-0.01 ± 0.09	0.00
2	-0.36 ± 0.05	-0.62 ± 0.05	-0.70 ± 0.05	-0.43 ± 0.08	-0.07 ± 0.08	0.00
3	$+0.82 \pm 0.05$	$+0.38 \pm 0.05$	$+0.32 \pm 0.05$	$+0.76 \pm 0.08$	$+1.20 \pm 0.08$	1.10
4	-0.36 ± 0.05	$+1.10 \pm 0.05$	$+1.14 \pm 0.05$	-0.32 ± 0.08	-0.04 ± 0.08	0.00
5	$+5.34 \pm 0.05$	$+4.73 \pm 0.05$	$+0.13 \pm 0.05$	$+0.73 \pm 0.09$	$+1.09 \pm 0.09$	1.10

Table 2: Results of the measurement applied to simulated samples.

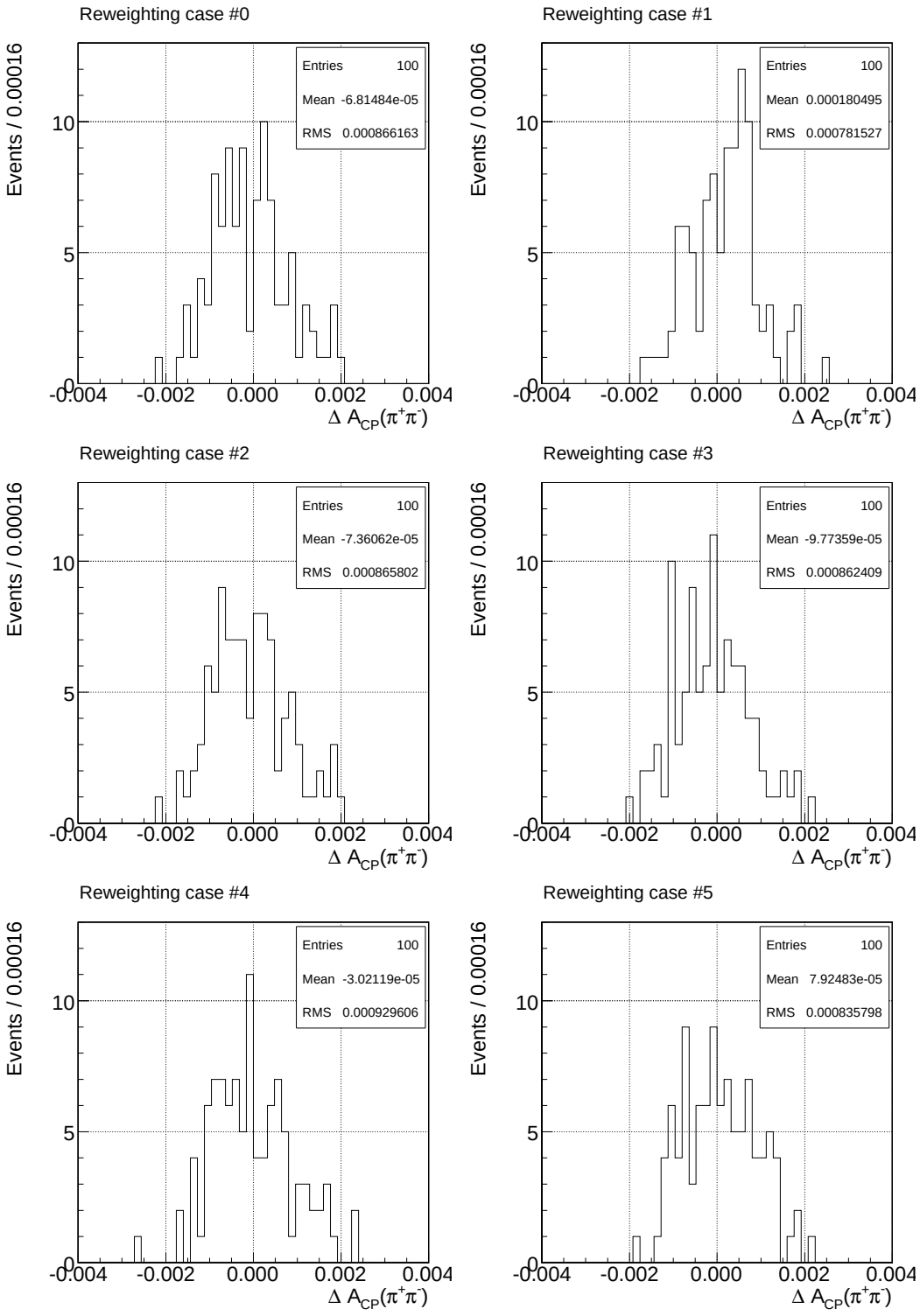

Figure 4: Distributions of the asymmetry bias for different cases.

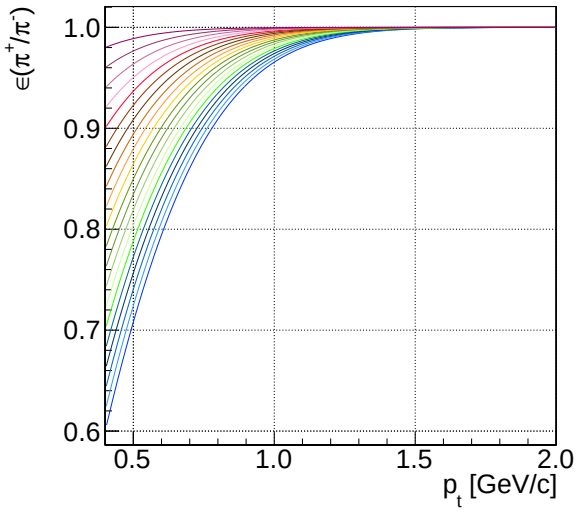

Figure 5: Curves corresponding to various ratios of efficiencies for reconstructing positive versus negative pions as a function of transverse momentum used to reweigh our samples.

To probe the domain of validity of our cancellation, we scan the value of a single input parameter across fairly large ranges starting from a given benchmark point. For each scan 21 different inputs are probed, which cover much larger variations than those expected in data from previous analyses:

- using eq. (6) for $\epsilon(\pi^+)/\epsilon(\pi^-)$, we vary the value of the constant A so that the efficiency ratio at 0.4 GeV/c spans from 60% to 100%, as shown in fig. 5;
- the ratio $\epsilon(K^+)/\epsilon(K^-)$ is changed from 60% to 100%;
- the physical $A_{\rm CP}(K\pi)$ from -10% to 10%;
- the physical $A_{\rm CP}(\pi\pi)$ from -10% to 10%.

We show the mean bias as a function of the input variables for case 0, in fig. 6, and for case 5, in fig. 7, as benchmark points. Each of the points in the plots is the mean value of the distribution of 1000 different tests.

Finally we tried one case with more realistic instrumental asymmetries.

- the p_T dependence of $\epsilon(\pi_s^+)/\epsilon(\pi_s^-)$ is taken fitting real data (fig. 2), the specific analitic expression used is

$$\frac{\epsilon(\pi^+)}{\epsilon(\pi^-)} = \mathrm{Erf}\,(2.49\ p_T) \tag{7}$$

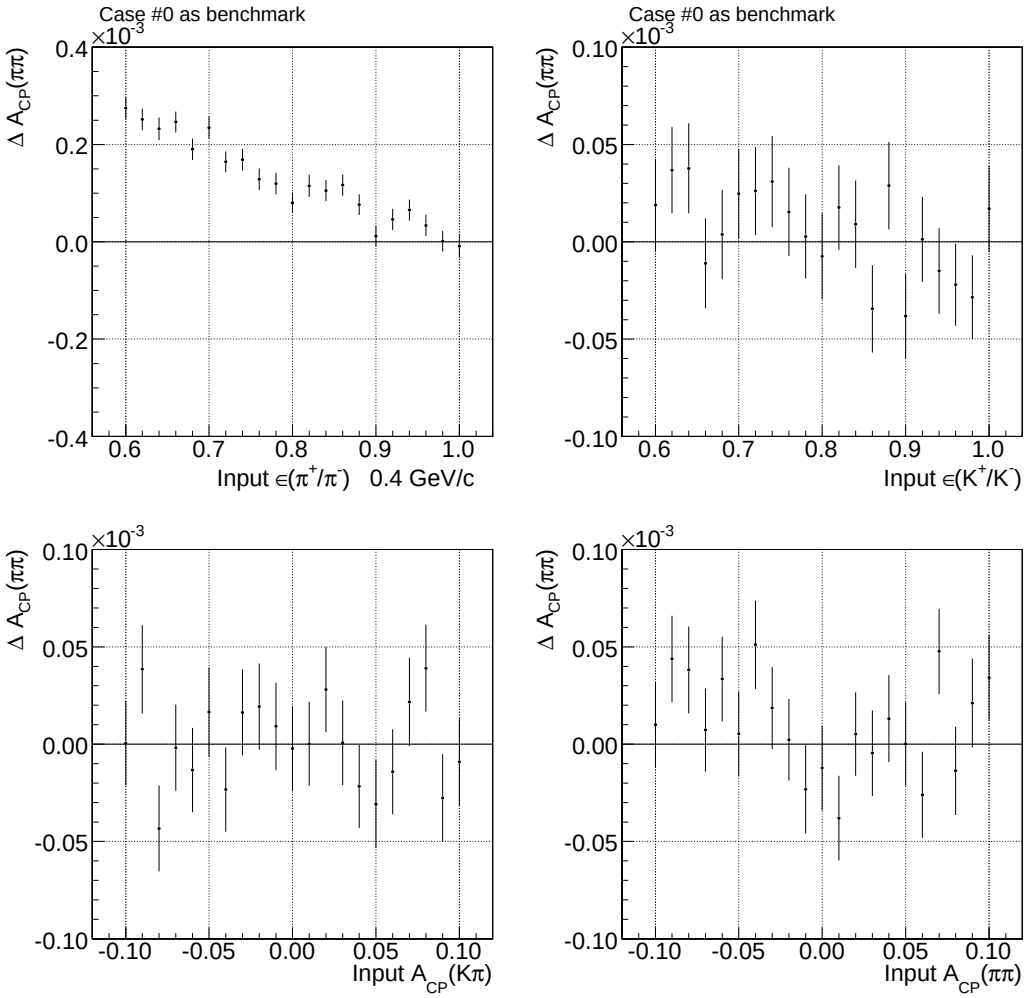

Figure 6: Asymmetry bias scans using case 0 as benchmark, which corresponds to a 10-fold resampling and no other inputs are varied except the quantities shown in each scan.

- we used $\epsilon(K^+)/\epsilon(K^-) \approx \epsilon(K^+\pi^-)/\epsilon(K^-\pi^+) = 1.0166$, where the approximation is valid assuming that for $p_T > 2$ GeV/c the efficiency for positive and negative pions is the same and the number is measured in [7];
- $A_{\rm CP}(K\pi) = 0.1\%$ that is at least two order of magnitude higher than the current theoretical upper limit and at least one order of magnitude higher than the current experimental sensitivity;
- and we scan on $A_{\rm CP}(\pi\pi)$ from -5% to 5% in steps of 0.5%.

The results are shown in fig. 8, the maximum observed bias is of the order of 0.01%, one order of magnitude smaller than the expected statistical resolution on the final measurement.

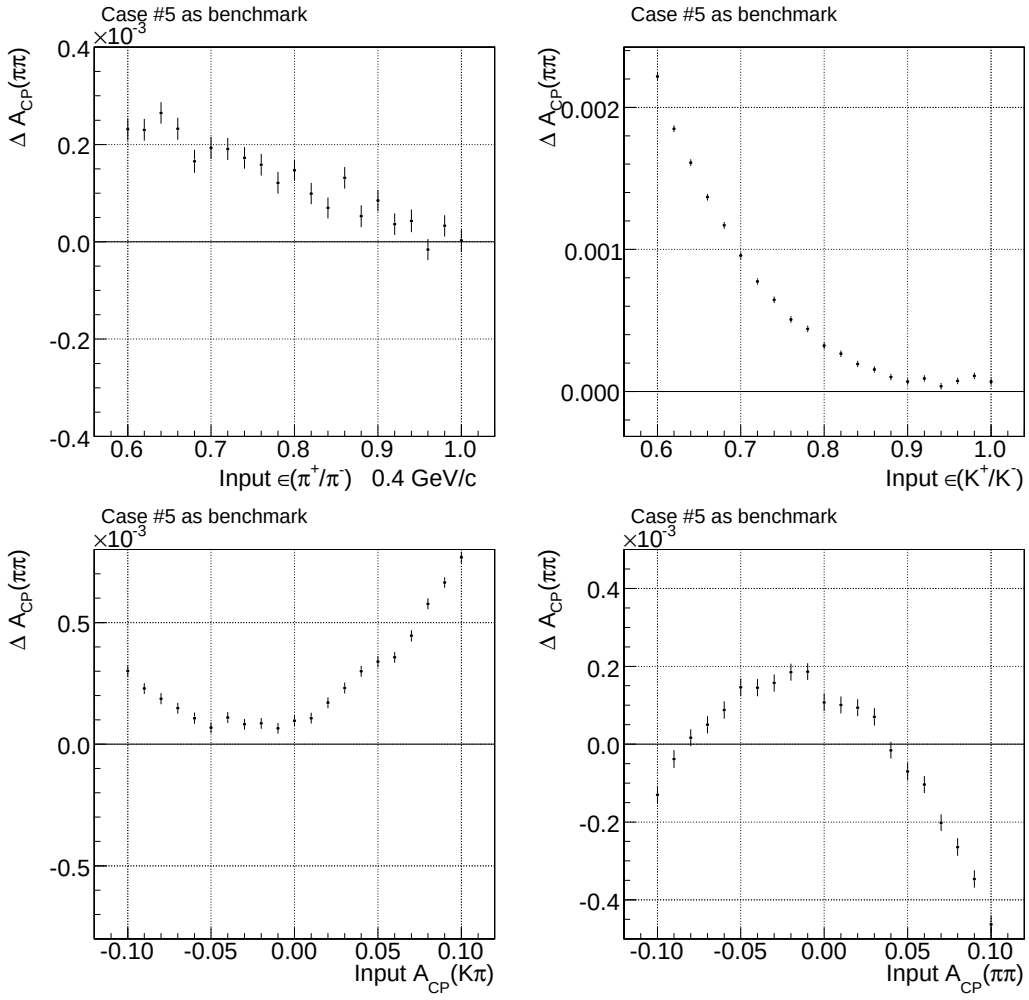

Figure 7: Asymmetry bias scan using case 5 as benchmark, which corresponds to a 10-fold resampling and inputs other than the quantities shown in the scan are set to be: $\epsilon(\pi^+/\pi^-)$ given by eq. (6) with value 80% at 0.4 GeV/c, $\epsilon(K^+/K^-) = 98\%$, $A_{\rm CP}(K\pi) = 0.8\%$ and $A_{\rm CP}(\pi\pi) = 1.1\%$.

3.4 Interpretation of results and conclusions

We tested the method proposed in [4] to measure $A_{\rm CP}(D^0 \to \pi^+\pi^-)$ using MC samples with good results: the cancellation works at 0.01% level even with induced asymmetries bigger than in reality. In sec. 6.1 will use this value as a systematic uncertainty on the final measurement associated to the method we use to extract the "corrected" CP violating asymmetry. This makes us very comfortable that our technique works well and that we can achieve our goal to have a final number with a systematic uncertanty at the permille level.

The following part of the note describes how we apply this technique to real data.

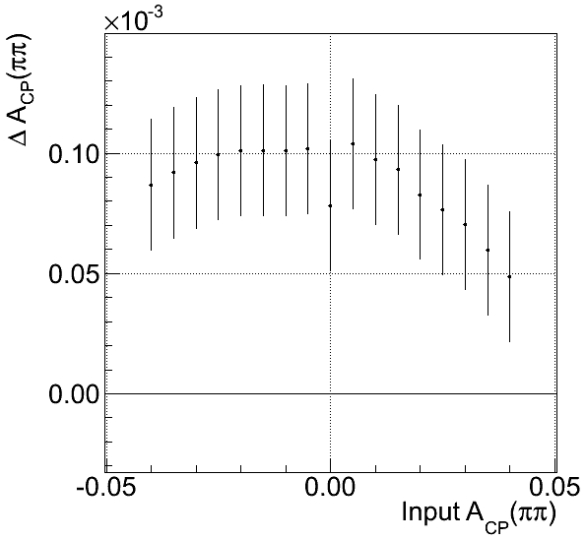

Figure 8: Asymmetry bias scan for a case with more realistic instrumental asymmetries: $\epsilon(\pi^+)/\epsilon(\pi^-)$ given by eq. (7), $\epsilon(K^+)/\epsilon(K^-) = 1.0166$, $A_{\rm CP}(K\pi) = 0.1\%$.

4 Datasets and reconstruction tools

The analysis described in this note uses the hadronic data sample collected with the Two Track Trigger. More specifically we a use part of the `B_CHARM` trigger paths family, as listed in tab. 3, that covers about 90% of the total available statistics. The details on how these trigger paths have been selected are reported in [8]. The analysis is performed starting from officially produced BStNtuples [6] available till P27 as summarized in tab. 4. A goodrun list version 33 with no requirements on calorimeter and muon bits is used. The integrated luminosity of our sample is approximately 5.94 fb^{-1}.

4.1 Candidates preselection

We skimmed the BStNtples to obtain smaller ntuples by reducing events of combinatorial background using a loose selection on the D^0 candidates.

We looked for $D^0 \to h^+h'^-$ candidates in the `B-PiPi` block selecting all events with at least one candidate that passes the following selection criteria (most of them already required at BStNtuple creation time):

- $1.2 \leqslant M(\pi\pi) \leqslant 2.4$ GeV/c^2, where $M(\pi\pi)$ is the invariant mass computed assigning the pion mass to both trigger tracks;
- $L_{xy}(D^0) \geqslant 0.02$ cm;

B_CHARM_LOWPT_	B_CHARM_	B_CHARM_HIGHPT_
L1_UPS[3]	L1_SCENA_LUMI_60[1]	DPS_L1_CLCM_LUMI_130[1]
L1_UPS[2]	L1_SCENA_UPS[1]	DPS_L1_CLCM[1]
L1_SCENLOW_PS2_LUMI_50[1]	L1_FPS[2]	L1_PS2[1]
L1_UPS[1]	L1_FPS[4]	DPS_L1_CLCM_LUMI_120[1]
L1_SCENLOW_LUMI_30[1]	L1_FPS[1]	L1_PS2_LUMI_70[2]
L1_SCENLOW_PS2_LUMI_40[1]	L1_FPS[3]	L1_PS2_LUMI_70[1]
L1_SCENLOW_LUMI_35[1]	L1_UPS[6]	L1_CLCM_DPS[8]
L1_PS2_LUMI_50[2]	L1_LUMI_80[5]	
	L1_LUMI_80[2]	
	L1_UPS[3]	
	NO_OPPQ_L1_LUMI_65[2]	

Table 3: List of trigger paths used in this analysis. The number in parenthesis is the version number.

Dataset	Period	Run range	Catalog location	Filesets
0d	0	138425-186598	cdfpbnt/xbhdid	1-503
0h	1-4	190697-203799	cdfpbnt/xbhdih	1-175
0i	5-10	203819-233111	cdfpbnt/xbhdii	1-272
0j	11-13	233133-246231	cdfpbnt/xbhdij	1-130
0k	14-17	252836-261005	cdfpbnt/xbhdik	1-117
0m	18-27	261119-287261	cdfpbnt/xbhdfm	24-334
0n	18	262870-263616	cdfpbnt/xbhdfn	1-14

Table 4: Details of BStNtuples used in the analysis.

- vertex quality $\chi^2 \leqslant 30$ and $\chi^2_{xy} \leqslant 15$;
- $q(1) \times q(2) < 0$;
- $|\boldsymbol{p}_t(1,2)| > 2$ GeV/c;
- $|\boldsymbol{p}_t(1)| + |\boldsymbol{p}_t(2)| \geqslant 4.5$ GeV/c;
- $|d_0(1,2)| \geqslant 0.007$ cm;
- $|\eta(1,2)| \leqslant 1.2$;
- $2^\circ \leqslant \Delta\phi \leqslant 90^\circ$

For each D^0 candidate we looped on the tracks in the `Pions` block looking for a soft pion to form a $D^\star \to D^0\pi_s$ candidate. We chose not to do a three-tracks vertex fit of the two

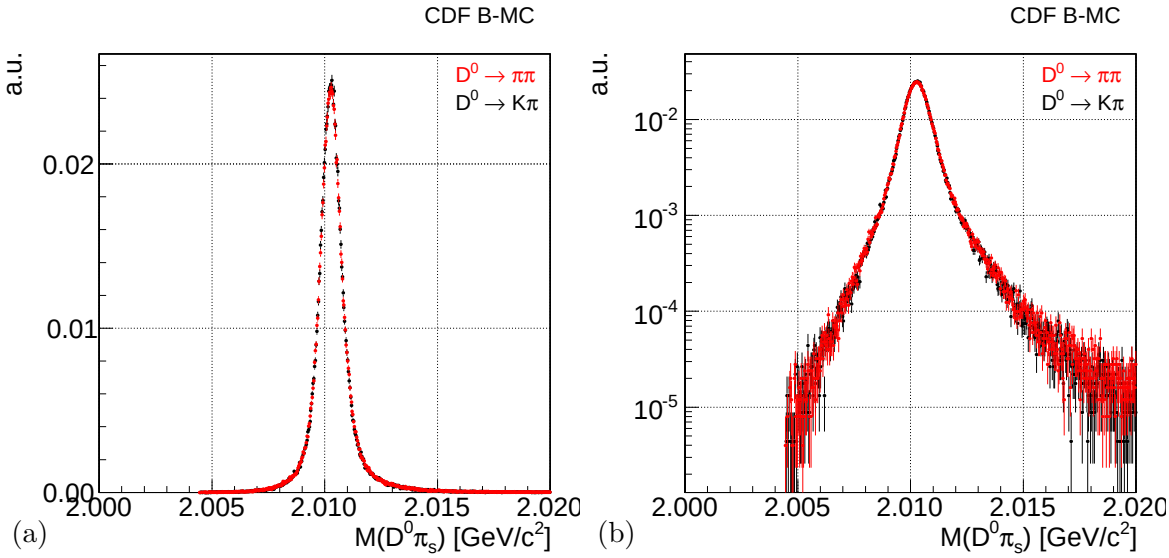

Figure 9: Comparison between the invariant $D^0\pi_s$-mass distributions of a B-MC sample of $D^\star \to D^0\pi_s$ with the $D^0 \to \pi\pi$ (red) and $D^0 \to K\pi$ (black) in linear (a) and log scale (b).

tracks from the neutral meson candidate and the soft pion. Since the soft pion has degraded resolution on track parameters with respect to the two 2 GeV/c tracks, we checked that little, if any, benefit would result from a full vertex fit. We therefore just associate the pion to the charm candidate with simple requirements on relative longitudinal and transverse separation. We only kept candidates with invariant $D^0\pi_s$-mass, $M(D^0\pi_s)$, less than 2.05 GeV/c^2, which will retain all possible $D^\star$ decays and provides enough sideband events to observe the background distribution.

We use the variable $M(D^0\pi_s)$, i.e. the invariant mass computed assigning the D^0 mass to the candidate formed with the two trigger tracks and the pion mass to the soft track, instead of the more usual difference between the reconstructed $D^\star$ and D^0 mass [2] [3]. Even if largely equivalent to the mass difference, this variable has the additional advantage that no mass hypothesis is needed for the D^0 tracks. Therefore all $D^0 \to h^+h'^-$ modes have the same $D^\star$ mass distribution, as shown in fig. 9.

4.2 Final selection cuts

In this first iteration of this analysis we did not devised a full optimization of the selection. Owing to large event statistics and high signal purities already after offline confirmation of the trigger cuts, we do not expect significant benefits from a dedicated optimization. Rather, we chose a selection inclusive enough to keep the large statistics available adding just some standard requirements for the soft pion. As a final requirements we select just D^0 candidates that pass the trigger confirmation, as explained in [8], and that further match the following

criteria:

- each candidate has to be associated with a reconstructed primary vertex;
- $|\eta(D^0)| \leqslant 1$;
- $|d_{xy}(D^0)| \leqslant 0.01$ cm, to remove most part of not promptly produced D^0s;
- $|\eta(1,2)| \leqslant 1$
- $|\boldsymbol{p}_t(1,2)| \geqslant 2.2$ GeV/c
- $0.01 \leqslant |d_0(1,2)| \leqslant 0.1$ cm
- # COT hits $(1,2) \geqslant 40$ and # COT Ax/St hits $(1,2) \geqslant 10$
- # Si ϕ hits $(1,2) \geqslant 3$, # Si 90 hits $(1,2) \geqslant 2$ and # Si SA hits $(1,2) \geqslant 1$

To remove most part of not-prompt background tracks we require soft pions associated to $D^\star$ candidates to pass the following selection:

- $|z_0(\pi_s)| \leqslant 1.5$ cm
- $|d_0(\pi_s)| \leqslant 0.06$ cm
- $|p_T(\pi_s)| \geqslant 0.4$ GeV/c
- $|\eta(\pi_s)| \leqslant 1$
- # COT hits $(\pi_s) \geqslant 30$
- # Si hits $(\pi_s) \geqslant 3$

We also studied the possibility to use PID information (dE/dx and TOF) to further clean our sample but any real gain in purity can be achieved from that (remember that dE/dx is not calibrated for tracks with transverse momentum below 2 GeV/c and just about 50% of the tracks are associated to a TOF measurement) so we decided to do not use PID in our analysis.

4.3 Multiple candidates removal

Multiple D^0 and $D^\star$ candidates may be present in the sample for various instrumental and physics reasons. Since we do not know the effects of our cancellation method in case of fake multiple candidates per event, and even a small fraction of events where the cancellation is ineffective can spoil our goal of permille precision, we studied the contamination of fake multiple candidates in our samples and removed them, as described in the following subsections.

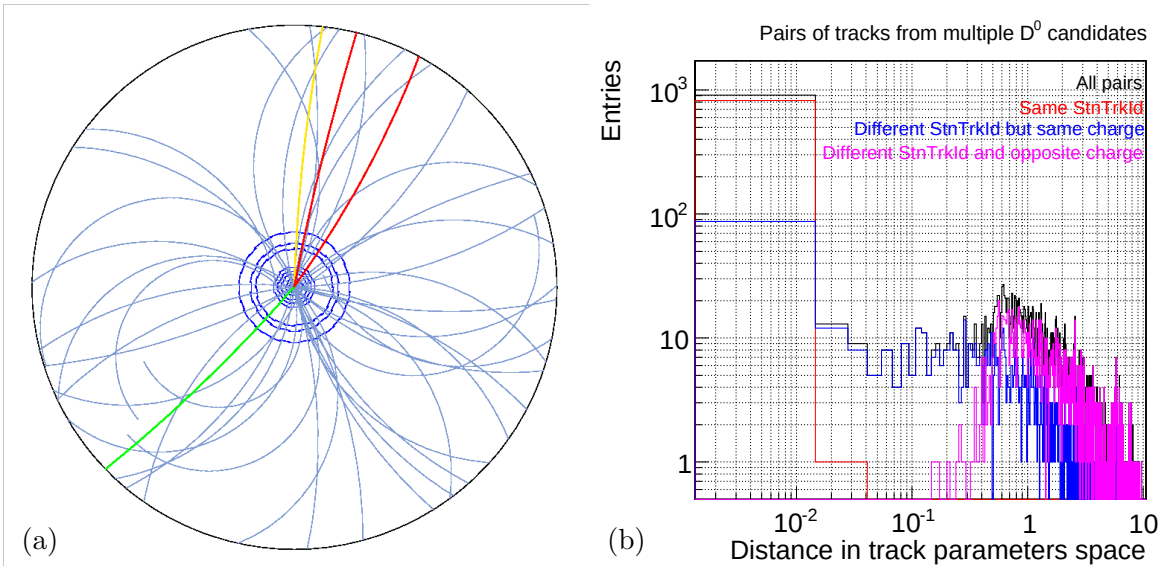

Figure 10: (a) COT display of reconstructed tracks for run 186352 event 1739942, two D^0 candidates are highlighted, each candidate is formed with a red and a yellow track. (b) Distribution of the distance in track parameters (eq. (8)) for pairs of tracks from multiple D^0 candidates with $|M(\pi\pi) - m_{D^0}| < 24$ MeV/c^2.

4.3.1 Multiple D^0 candidate events

After trigger confirmation and final selection cuts our sample contains $\sim 310 \times 10^3$ events with more than one D^0 candidate and $\sim 103 \times 10^6$ with just one. This fraction ($f_{mc} \sim 4 \times 10^{-4}$ around the $D^0 \to \pi\pi$ peak) is larger than what we expect.

Studying the topology of such candidates and their distribution in the tracking volume we realized that a non negligible part of them were due to candidates that have a track in common with a different candidate of the same event. Fig. 10 (a) shows an example. To eliminate this ambiguity we decided to choose just one candidate, the one with the lowest χ^2, and remove the others from our sample. To do that we assumed that two reconstructed tracks are associated to the same charged-particle trajectory if

- they have the same StnTrkId (the identification number associated to each track in the BStNtuple) or
- they have the same charge and the Euclidean distance in the track parameters space,

$$d(t_1, t_2) = \sqrt{\Delta p_T^2 + \Delta\eta^2 + \Delta\phi_0^2 + \Delta z_0^2 + \Delta d_0^2}, \tag{8}$$

  is less than 0.02.

Fig. 10 (b) shows the distribution of this distance for a sample of multiple D^0 candidates with $|M(\pi\pi) - m_{D^0}| < 24$ MeV/c^2. The distribution of the total number of D^0 candidates

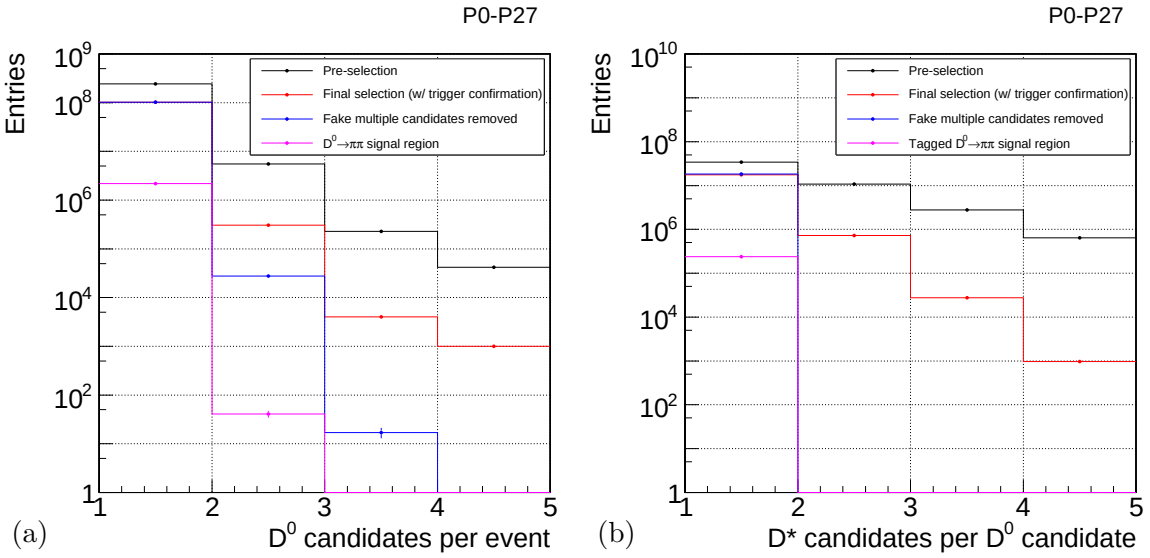

Figure 11: Distribution of multiple D^0 (a) and $D^\star$ (b) candidates at different stages of our selection.

per event before and after this multiple candidates removing procedure is shown in fig. 11 (a): after removing fake multiple candidates the ratio f_{mc} becomes $\sim 1.9 \times 10^{-5}$.

4.3.2 Multiple $D^\star$ candidate events

A different approch is used for multiple $D^\star$ candidate events. Fig. 11 (b) shows the distribution of the number of $D^\star$ candidates per D^0 candidate present in our sample. After our final selection we have a fraction of $\sim 2.2\%$ of cases in which for a single D^0 candidate there is more than one soft track available to form a $D^\star$ candidate. By construction only one of these candidates could be a real $D^\star$, the others should be fake.

Looking at the distribution of the distance of track parameters, as defined in eq. (8), calculated for each pair of tracks that are from multiple $D^\star$ candidates with $|M(\pi\pi) - m_{D^0}| < 24$ MeV/c^2 and $|M(D^0\pi_s) - m_{D^\star}| < 2.4$ MeV/c^2 we found that about 23% of these events are due to duplicated tracks ($d < 0.02$) and that the occurence of duplicated tracks is more than 80% for transverse momenta in the range $0.4 - 0.45$ GeV/c, as shown in fig. 12. More likely these are tracks reconstructed with different tracking algorithms that overlap in that transverse momenta interval.

Furthermore there are events in which both a positive and a negative soft pion are associated to the same D^0 candidate, i.e. in these cases we completely loose the tagging power provided by the strong $D^\star$ decay.

Since it is not clear how to eliminate the ambiguity that comes from these kind of events we decided, to avoid any possible bias, to choose randomly only one candidate whenever there

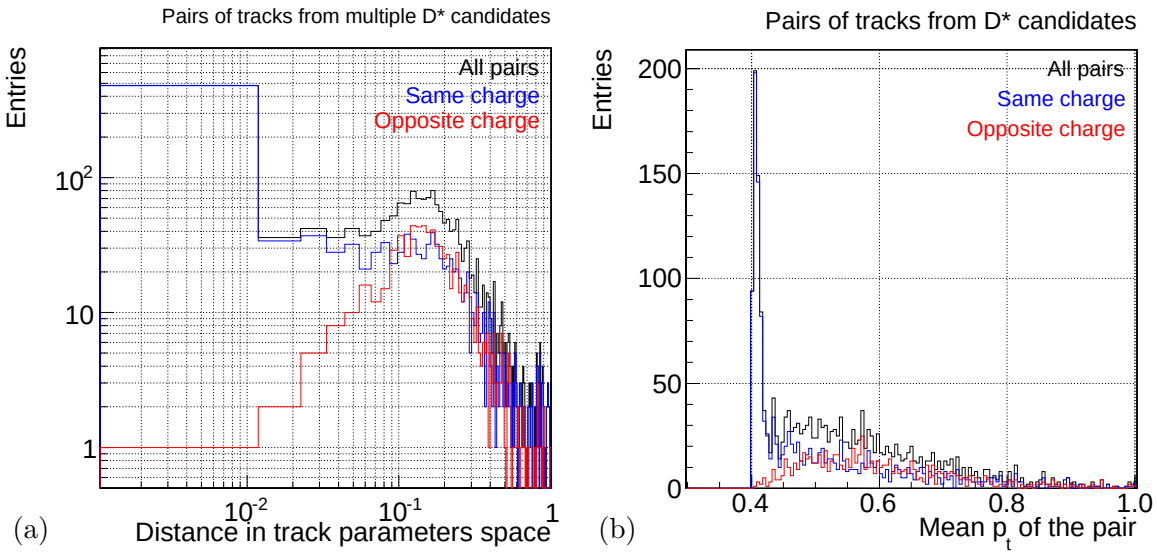

Figure 12: Distribution of distance in track parameters (eq. (8)) (a) and mean transverse momentum (b) for pairs of tracks from multiple $D^\star$ candidates with $|M(\pi\pi) - m_{D^0}| < 24$ MeV/c^2 and $|M(D^0\pi_s) - m_{D^\star}| < 2.4$ MeV/c^2.

were events with multiple $D^\star$ candidates per D^0 candidate.

4.4 Tagged $D^0 \to K^-\pi^+$ and $D^0 \to \pi^+\pi^-$ samples

The selection described so far is common to all tagged and untagged $D^0 \to h^+h'^-$ decays. Sample-specific mass requirements to select a pure signal in each of the two different tagged samples ($D^0 \to \pi\pi$ and $D^0 \to K\pi$ decays) used in this measurements are described in the following. The measurement of the untagged $D^0 \to K\pi$ uncorrected asymmetry is exhaustively described in [9]. In this document we focus on the measurement of the uncorrected asymmetries in these tagged channels and on the extraction of the physics asymmetry.

In addition to the requirements of sec. 4 we select the two tagged samples requiring the two-body mass ($M(K\pi)$ for the $D^0 \to K\pi$ case and $M(\pi\pi)$, for the $D^0 \to \pi\pi$ case) to lie within about 3σ of the nominal D^0 mass ($|M(hh') - m_{D^0}| \leqslant 24$ MeV/c^2) as shown in figs. 13 (a)–(b). The same figure also shows the $M(D^0\pi_s)$ distribution for the two samples after this requirement is applied. Note how clean the $D^\star$ peak is in both tagged samples, even if no optimization was performed to extract the signal.

4.4.1 Reweighting of π_s distributions

The technique for suppressing detector-induced asymmetries in soft pion reconstruction is supposed to work with desired accuracy only if the kinematics of the π_s in the two tagged

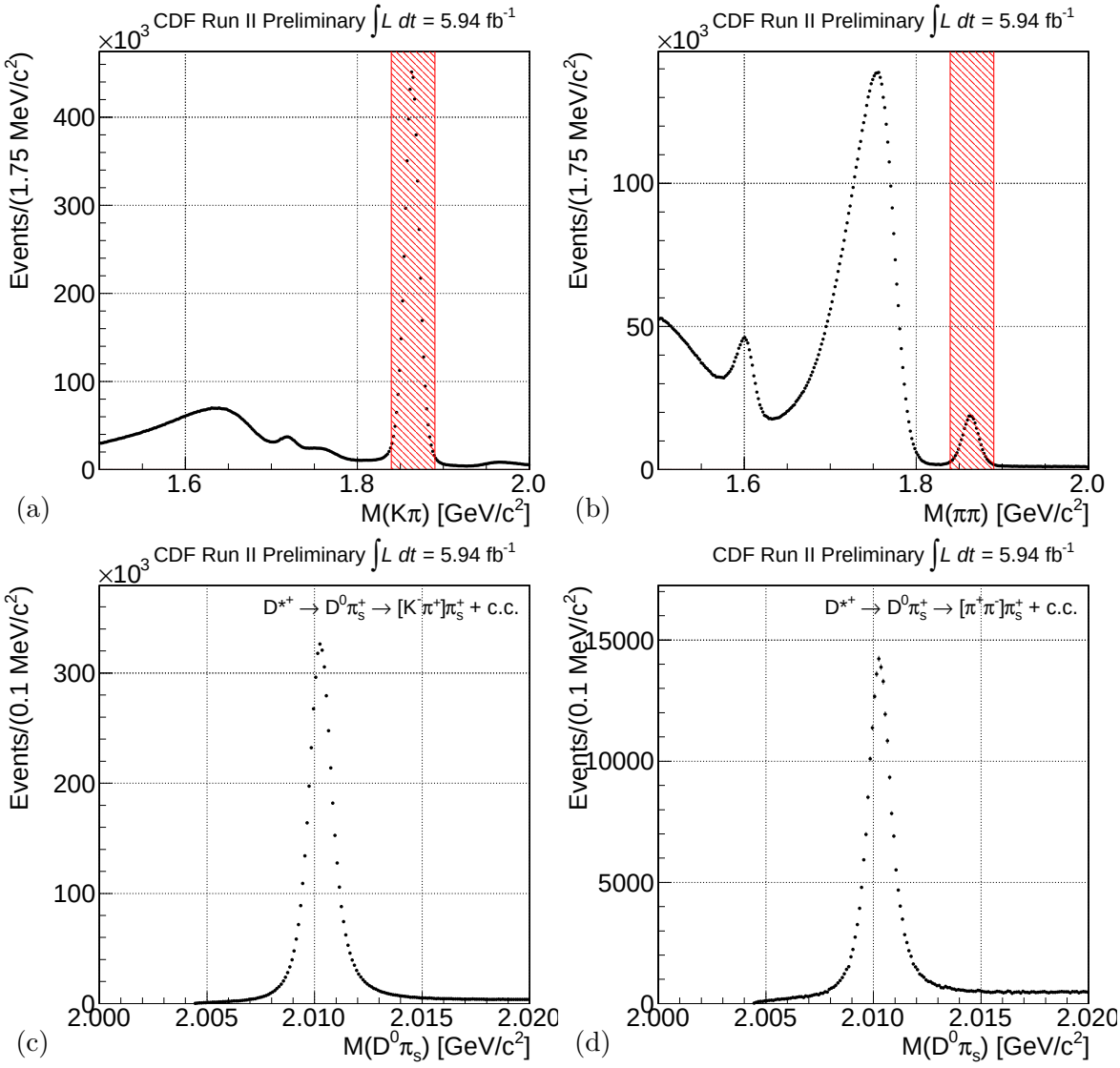

Figure 13: $M(K\pi)$ (a) and $M(\pi\pi)$ distributions (b) with regions used to define the two tagged samples highlighted in red. $M(D^0\pi_s)$ distribution for the tagged $D^0 \to K\pi$ (c) and $D^0 \to \pi\pi$ (d) samples selected in the two red regions.

samples is the same[1]. Small differences between soft pion distributions associated to decays in different D^0 final states ($K\pi$ or $\pi\pi$) may be possible due to trigger and reconstruction biases. We checked for them and when necessary we reweighed the tagged $D^0 \to \pi\pi$ sample so that soft pion's distributions look the same as in the tagged $D^0 \to K\pi$ one.

[1]Remember the approximation $\delta(\pi_s)^{\pi\pi^\star} \approx \delta(\pi_s)^{K\pi^\star}$ used to extract the final formula in eq. (5).

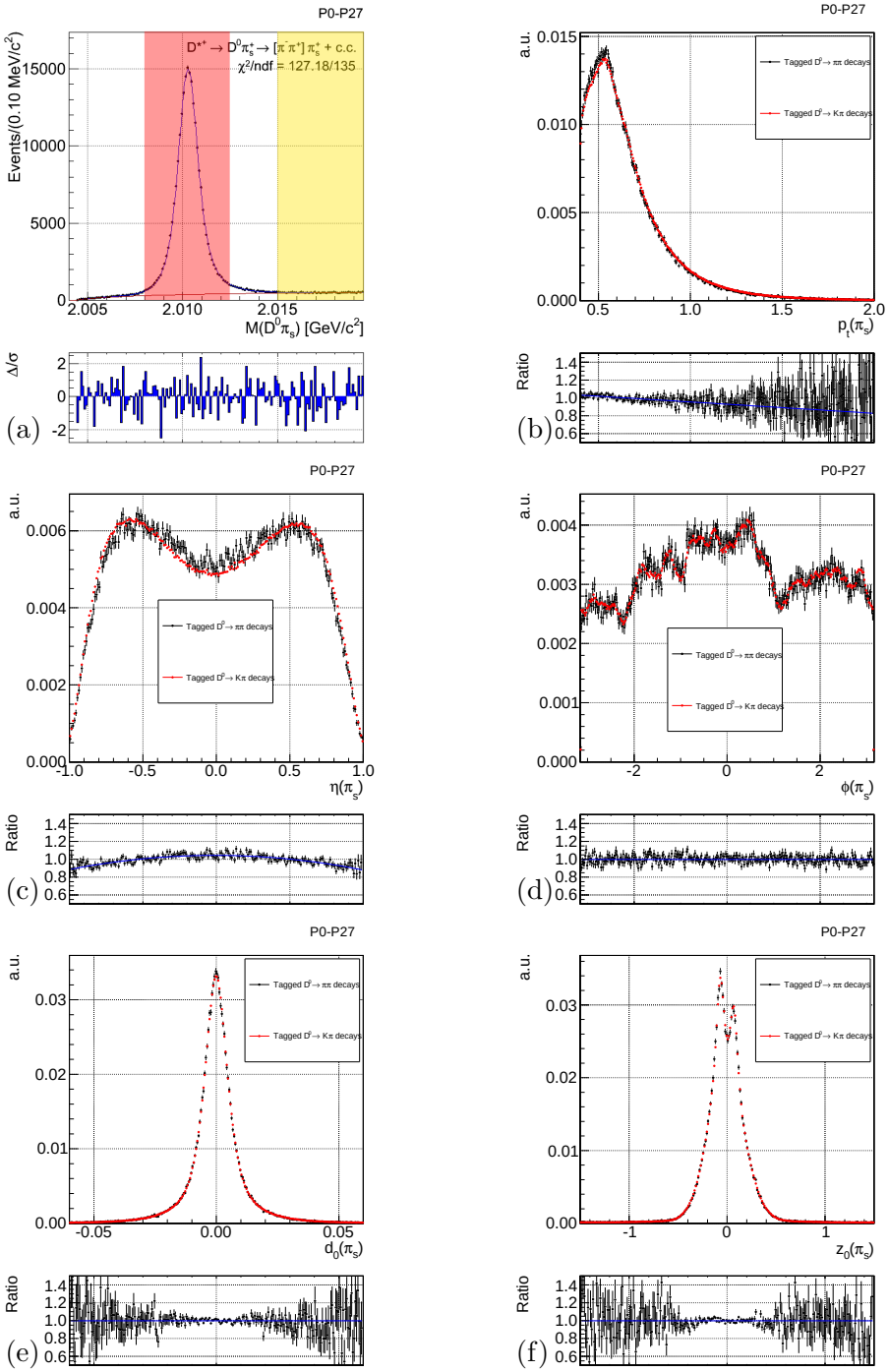

Figure 14: Invariant $D^0\pi_s$-mass distribution with highlighted the signal (red band) and background (yellow band) regions (a) used in the sideband subtraction procedure to compare transverse momentum (b), pseudo-rapidity (c) azimuthal angle (d), impact parameter (e) and z_0 coordinate (f) distributions of soft pion tracks in the two tagged samples.

We define a signal region around the $D^\star$ peak and sideband region at higher $M(D^0\pi_s)$ values as represented in fig. 14 (a). Then we compare normalized sideband-subtracted distributions for tagged $\pi\pi$ and tagged $K\pi$ sample. We study a large set of π_s kinematic variables (p_T, η, ϕ, d_0 and z_0) and we observe small discrepancies only in p_T and η distributions as shown in fig. 14. We fit the ratio between the two histograms and we use the product of the two resulted functions to estract the weight for the $D^0 \to \pi\pi$ tagged sample, i.e. we assume that the two effects are indipendent: weight(tot) = weight(p_t) $\times$ weight(η)[2].

All distributions shown in the following sections are reweighed in transverse momentum and pseudo-rapidity as described above, unless otherwise stated.

4.4.2 The asymmetry as a function of mass

Fig. 15 shows the uncorrected CP asymmetry as a function of $D^0\pi_s$-mass. This is obtained by determining, in each mass bin, the asymmetry between the event yield of $D^{\star+}$ candidates (h_+) and $D^{\star-}$ candidates (h_-):

$$h_{\rm a} = \frac{h_+ - h_-}{h_+ + h_-}.$$

This plot is a direct representation of the measured quantity. The projection of the combined fit result on this view, as we will see in the following sections, is a powerful cross check of the quality of the entire procedure.

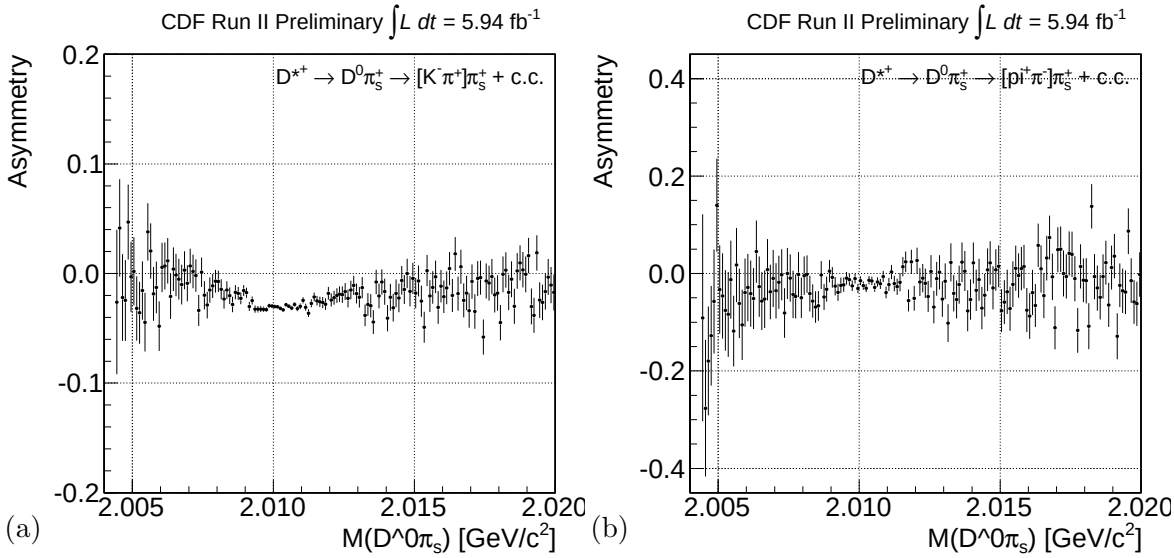

Figure 15: Uncorrected raw asymmetry as a function of the invariant $D^0\pi_s$-mass for the tagged $D^0 \to K\pi$ (a) and $D^0 \to \pi\pi$ (b) samples.

[2]We verified *a posteriori* that this assumption is a good approximation.

5 Fit of tagged samples

Fig. 13 shows that the CDF II tracker provides enough mass resolution to separate the different D^0 decay modes we are interested in from any other physical background. As a consequence our samples have high purity and the only source of background comes from random pions associated to a real D^0 candidate. To subtract this background all the information we need is in the invariant $D^0\pi_s$-mass. A fit of this distribution for positive and negative $D^\star$s determines events yields and can be used to compute the uncorrected asymmetries on the two tagged samples that enter in eq. (5).

A joint binned fit to the $M(D^0\pi_s)$ distribution combining $D^{\star+}$ and $D^{\star-}$ decays in both tagged samples is done to minimize a combined χ^2 quantity, defined as

$$\chi^2_{\rm tot} = \chi^2_+ + \chi^2_-,$$

where χ^2_+ and χ^2_- are the individual chi-squared for the two distributions. The functional form that describes the $M(D^0\pi_s)$ shape is assumed to be the same for both charges but individual parameters can be let free to float and adjust themselves independently for positive and negative charges. This aspect will be further discussed in the determination of systematic uncertainties.

5.1 Templates

The CDF II simulation does not reproduce with enough accuracy the $M(D^0\pi_s)$ shape. We extracted the signal template to be used in the fit directly from data: we use the B-MC sample of $D^{\star+} \to D^0\pi_s^+ \to [K^-\pi^+]$ decays just to determine the starting value of our signal template and then we fit data to extract the template used in the combined fit. Since at this stage we are not interested in possible differences between the two charges we extract the signal shape fitting the summed histogram,

$$h_{\rm s} = h_+ + h_-.$$

The signal lineshape is well described by a Johnson function,

$$J_{\rm SU}(x|\mu,\sigma,\delta,\gamma) = \frac{1}{\rm Norm}\ \frac{e^{-\frac{1}{2}\left[\gamma+\delta\sinh^{-1}\left(\frac{x-\mu}{\sigma}\right)\right]^2}}{\sqrt{1+\left(\frac{x-\mu}{\sigma}\right)^2}},$$

that accounts for the asimmetric tail of the distribution, plus two Gaussians,

$$G(x|\mu,\sigma) = \frac{1}{\rm Norm}\ e^{-\frac{1}{2}\left(\frac{x-\mu}{\sigma}\right)^2},$$

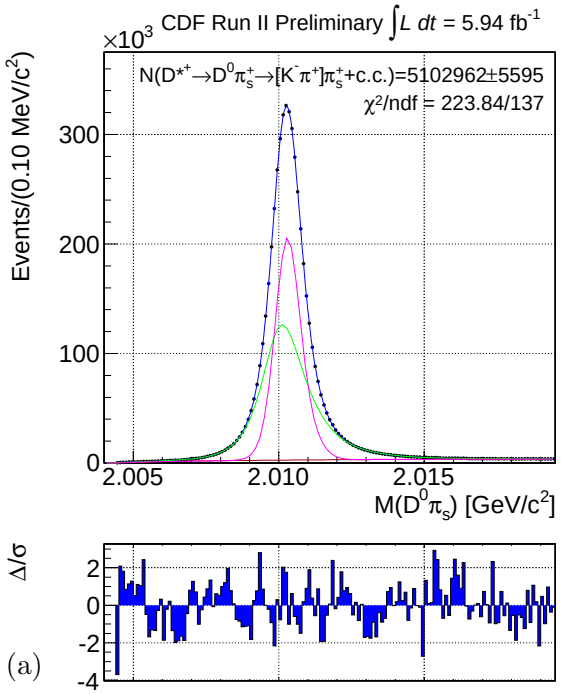

(a)

PARAMETER	FITTED VALUE	NOTES
$N_{\rm sgn}$	5102962 ± 5595	
f_J	0.54 ± 0.04	
μ_J	$(-3.3 \pm 0.2) \times 10^{-4}$	
σ_J	$(-9.8 \pm 0.7) \times 10^{-4}$	
γ_J	-0.38 ± 0.02	
δ_J	1.14 ± 0.02	
f_{G1}	0.58 ± 0.02	
μ_{G1}	$(3 \pm 8) \times 10^{-6}$	
σ_{G1}	$(3.92 \pm 0.06) \times 10^{-4}$	
μ_{G2}	$(1.8 \pm 0.3) \times 10^{-4}$	
σ_{G2}	$(6.0 \pm 0.1) \times 10^{-4}$	
$N_{\rm bkg}$	409699 ± 5160	
b	0.66 ± 0.01	
c	34 ± 3	
threshold (a)	$m_{D^0} + m_\pi$	fixed

(b)

Figure 16: Results from the preliminary fit on the tagged $D^0 \to K\pi$ sample (both charges together) aimed to extract signal shape template to be used in the combined fit. The total fit projection (blue) on $M(D^0\pi_s)$ distribution is shown in (a) with overlayed all the components of shape: the double Gaussian bulk (magenta), the Johnson tail (green) and the background (red). The resulted fitted parameters are in table (b).

for the central bulk:

$$\begin{aligned}\mathrm{PDF}_{\rm sgn}(x) = f_J J_{\rm SU}(x|m_{D^\star} + \mu_J, \sigma_J, \delta_J, \gamma_J) \\ + (1 - f_J)\,[f_{G1} G(x|m_{D^\star} + \mu_{G1}, \sigma_{G1}) \\ + (1 - f_{G1}) G(x|m_{D^\star} + \mu_{G2}, \sigma_{G2})]\end{aligned}$$

For the background we use the following as an empirical form

$$\mathrm{PDF}_{\rm bkg}(x) = \frac{1}{\mathrm{Norm}}\ (x - a)^b e^{-c(x-a)},$$

so that the total function used in this preliminary fit is

$$\mathrm{F}[M(D^0\pi_s)] = N_{\rm sgn}\mathrm{PDF}_{\rm sgn}[M(D^0\pi_s)] + N_{\rm bkg}\mathrm{PDF}_{\rm bkg}[M(D^0\pi_s)]$$

Note that each PDF is truncated at the threshold value of $m_{D^0} + m_\pi$.

Fig. 16 shows the result obtained fitting data: all parameters are freely to float in the fit with the only exception of a that is fixed to the threshold value.

Using this data-driven parameterization, we fit simultaneously the $M(D^0\pi_s)$ distributions of $D^{\star+}$ and $D^{\star-}$ and extract the asymmetry. In this combined fit we leave background parameterization free to vary, under the assumption that the functional form is the same for both negative and positive samples, while in principle signal parameterization could be different. To reduce sensitivity to the statistical fluctuations of the tagged $\pi\pi$ sample, we fix the $M(D^0\pi_s)$ signal shape in the tagged $D^0 \to \pi\pi$ fit to the one obtained fitting the higher statistics tagged $K\pi$ sample. This is justified because the $M(D^0\pi_s)$ distribution obtained using the nominal mass is independent of the specific $D^0 \to h^+h'^-$ decay, once soft pion distributions have been equalized.

5.2 Fit results

Fig. 17 shows the best fit result for the tagged $D^0 \to K\pi$ sample: the table reports all the parameters that are left free in the fit, the others are fixed to the value obtained in the preliminary fit (fig. 16).

We tried to force both positive and negative signal shape parameters to be the same but we observed that leaving δ_J to vary indipendently for positive and negative decays the χ^2/ndf value improves from 414/306 to 386/304 and the total fit projection gives a better description of the asymmetry as a function of the invariant $D^0\pi_s$-mass in the range $[2.008, 2.010]$ GeV/c^2. Leaving other signal shape's parameters free to vary independently for $D^{\star+}$ and $D^{\star-}$ does not improve the fit quality significantly. Small differences between positive and negative signal shapes may be expected since the COT has different resolutions for positive and negative low momentum tracks. We don't expect the source of this difference to be the background, since the difference is visibile essentially in the signal region, where the correlation between $D^0\pi_s$-mass and π_s transverse momentum is stronger. As explained in sec. 6.2 we will quote a systematic error associated to that assumption.

Fig. 18 shows the best fit result for the tagged $D^0 \to \pi\pi$ sample. As already stated we fix the signal parameterization to the one obtained fitting the tagged $K\pi$ sample (fig. 17) while all background parameters are left free to float.

The uncorrected asymmetries we evaluate from the two tagged samples are then:

$$A_{\rm CP}^{\rm raw}(K\pi^\star) = (-2.910 \pm 0.049)\% \quad \text{and} \quad A_{\rm CP}^{\rm raw}(\pi\pi^\star) = (-1.86 \pm 0.23)\%$$

Combining, as in eq. (5), these two numbers with the raw asymmetry measured in the untagged $D^0 \to K\pi$ sample [9] (and considering just the statistical uncertainties for now) we

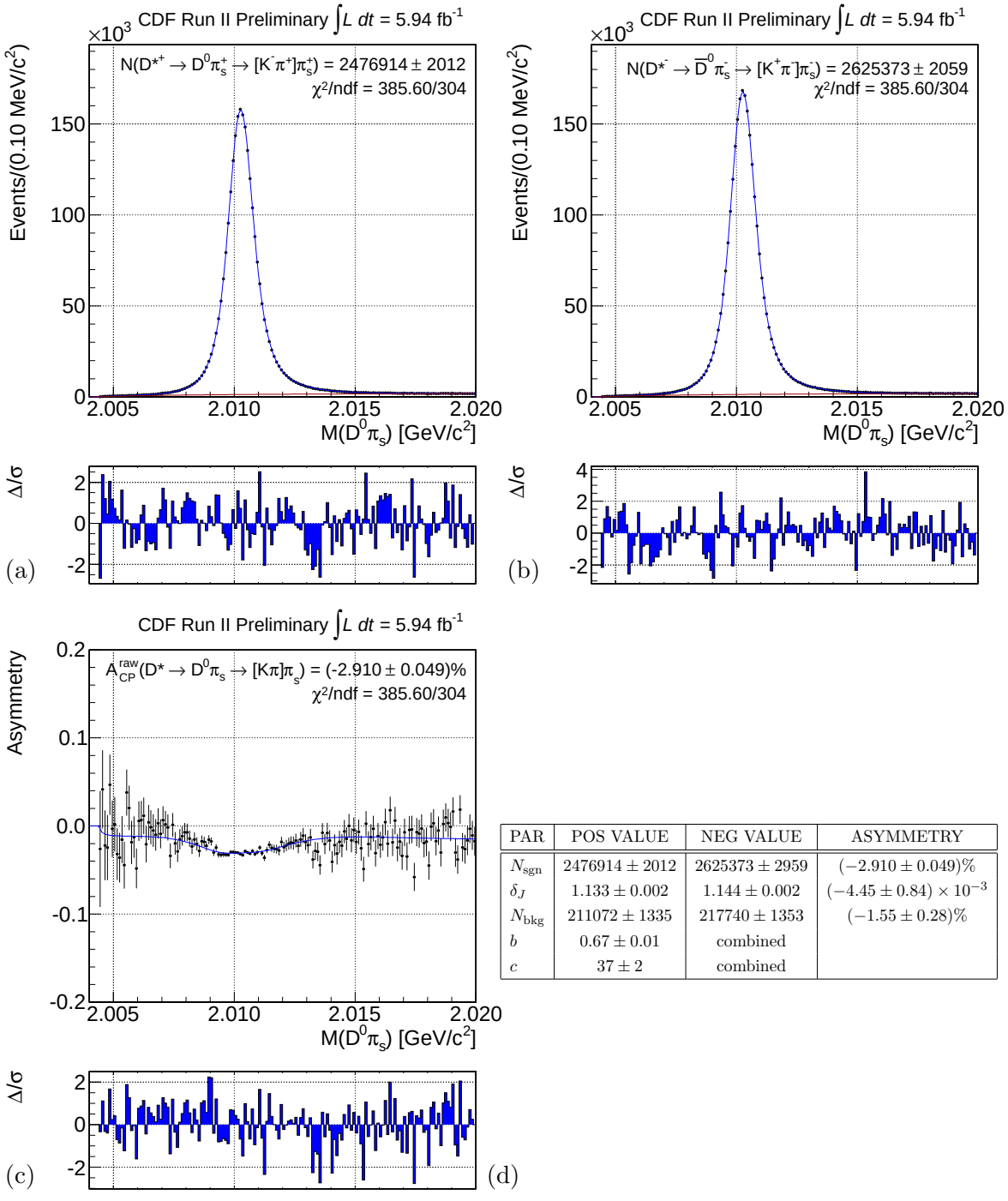

PAR	POS VALUE	NEG VALUE	ASYMMETRY
$N_{\rm sgn}$	2476914 ± 2012	2625373 ± 2959	$(-2.910 \pm 0.049)\%$
δ_J	1.133 ± 0.002	1.144 ± 0.002	$(-4.45 \pm 0.84) \times 10^{-3}$
$N_{\rm bkg}$	211072 ± 1335	217740 ± 1353	$(-1.55 \pm 0.28)\%$
b	0.67 ± 0.01	combined	
c	37 ± 2	combined	

Figure 17: Results from the combined fit on the tagged $D^0 \to K\pi$ sample. Fit projection on $M(D^0\pi^s)$ distribution for positive (a) and negative (b) decays and on the asymmetry as a function of $M(D^0\pi^s)$ (c). The fitted parameters are shown in table (d).

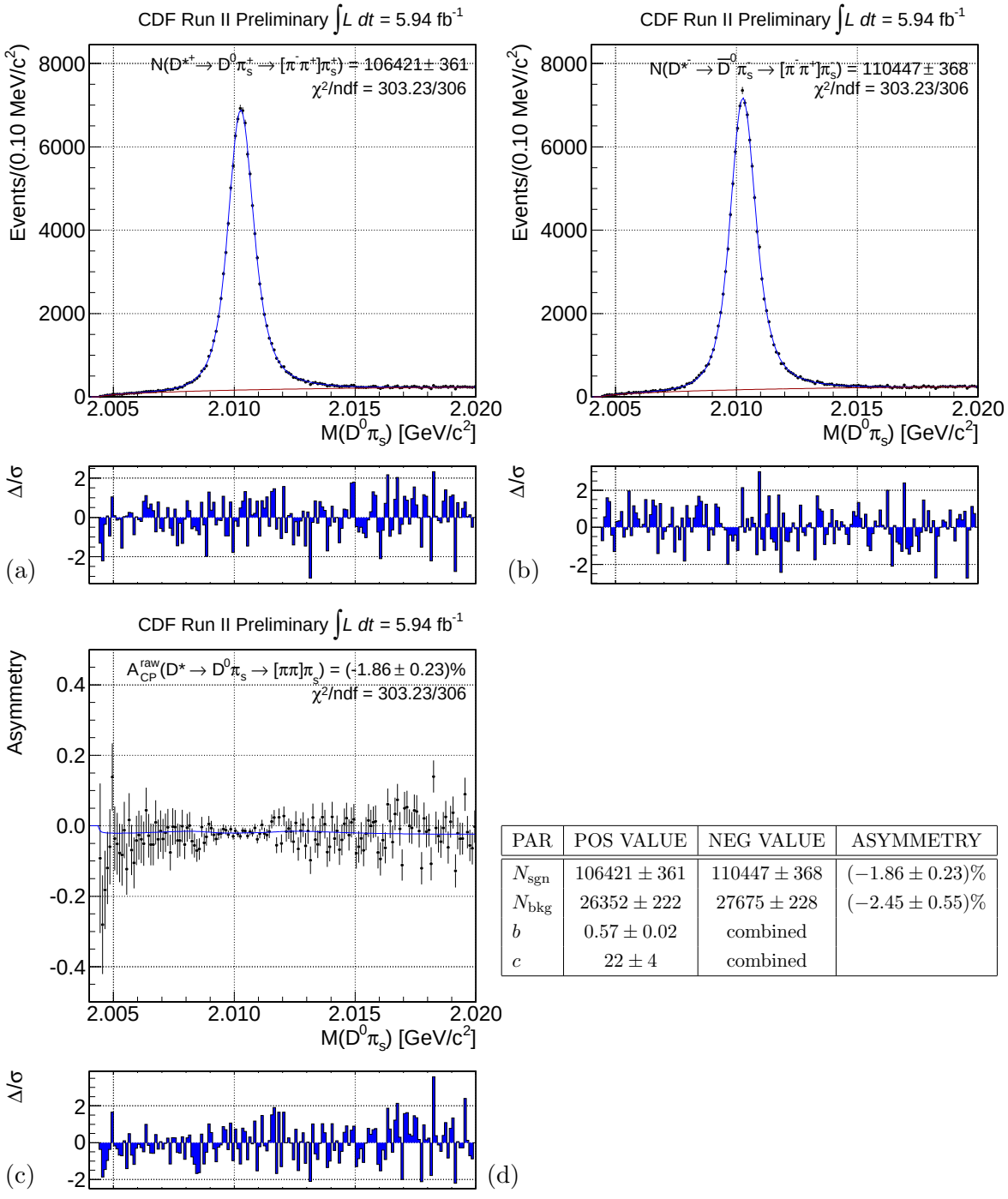

PAR	POS VALUE	NEG VALUE	ASYMMETRY
$N_{\rm sgn}$	106421 ± 361	110447 ± 368	$(-1.86 \pm 0.23)\%$
$N_{\rm bkg}$	26352 ± 222	27675 ± 228	$(-2.45 \pm 0.55)\%$
b	0.57 ± 0.02	combined	
c	22 ± 4	combined	

Figure 18: Results from the combined fit on the tagged $D^0 \to \pi\pi$ sample. Fit projection on $M(D^0\pi^s)$ distribution for positive (a) and negative (b) decays and on the asymmetry as a function of $M(D^0\pi^s)$ (c). The fitted parameters are just the ones shown in table (d).

found that the CP violating asymmetry in $D^0 \to \pi^+\pi^-$ decays is

$$A_{\rm CP}(\pi\pi) = A_{\rm CP}^{\rm raw}(\pi\pi^\star) - A_{\rm CP}^{\rm raw}(K\pi^\star) + A_{\rm CP}^{\rm raw}(K\pi) = \\ (-1.86 \pm 0.23)\% - (-2.91 \pm 0.05)\% + (-0.83 \pm 0.03)\% = \\ (+0.22 \pm 0.24)\%$$

As expected we have the possibilty to obtain the most precise measurement to date, with a statistical uncertainty that is about two times better than current B-factories results.

6 Systematic uncertainties

We consider the following sources of systematics.

- Effects from assumptions and approximations of the method. These affect directly the final, corrected $A_{\rm CP}(\pi\pi)$ result:
  1. factorization of $K\pi$ and π_s reconstruction efficiencies;
  2. non-cancellation of higher order instrumental asymmetries;
  3. beam drag effects;
  4. contamination of not promptly produced D^0 mesons.
- Systematic uncertainties affecting the uncorrected symmetries:
  1. effects of the specific choice of analytic shapes used in fits;
  2. effect of possible differences between distributions of quantities associated to a $D^{\star-}$ or $D^{\star+}$;
  3. effect of possible contamination from unexpected backgrounds;
  4. effect from finite accuracy of reweighting functions.

Since the size of the data samples used is very high we decided to evaluate most of the systematic uncertainties using the data itself. We modified the input to the fits to include systematic variations and repeated the fit on data. The difference between these and the central fit is taken as systematic uncertainty. This procedure is an overestimation of the size of the systematic effect because it introduces and additional, statistical source of fluctuation in the results. But we can comfortably afford that given the large event samples size involved. A summary of all systematic uncertainties is shown in tab. 6.

6.1 Assumptions and approximations in our method

6.1.1 Higher order effects and efficiency factorization ansatz

We checked the reliability of detector induced asymmetries cancellation by validating our method on simulation as described in sec. 3. These studies provide an upper limit on possible asymmetries induced by higher order non-cancelled detector effect and not factorization of $K\pi$ and π_s reconstruction efficiencies. Based on the results shown, we assess the maximum systematics from this source to be $\Delta A_{\rm CP}(\pi\pi) = 0.01\%$.

6.1.2 Beam drag effects

Color interactions may induce pseudorapidity-dependent asymmetries between the number of produced charm and anticharm mesons. One could imagine that charm mesons emitted closer to the beam and in the same direction may keep some residual "memory" of the underlying beam through color correlations/interference. To cancel charge asymmetries in D^0 and $D^\star$ production due to beam drag effects our method assumes that our acceptance is symmetric in pseudorapidity. The correction to $A_{\rm CP}(\pi\pi)$ due to this assumption, as described in [4], is of the order of the production charge asymmetry times the detector η asymmetry averaged over the acceptance. The detector η asymmetry is evaluated measuring the forward-backward asymmetry of the tagged $K\pi$ sample:

$$A_{\rm FB} = \frac{N(\eta > 0) - N(\eta < 0)}{N(\eta > 0) + N(\eta < 0)} = (1.15 \pm 0.05)\%.$$

Production charge asymmetry due to beam drag effects will result as a slope in charge asymmetry vs η. Fig. 19 show that this slope is measured to be $(-0.38 \pm 0.09)\%$. A systematic error has been assessed multiplying these two numbers: $\Delta A_{\rm CP}(\pi\pi) = 0.004\%$.

6.1.3 Non-promptly produced charm mesons

Our sample has a contamination from charm produced in b–hadron decays. Therefore their initial relative yields could be spoiled by physics asymmetries in b–hadron decays. These may be large for a single exclusive mode, but are expected to average to zero for inclusive $B \to DX$ decays. However we should assess a possible effect from this source. If D^0s come from B decays the asymmetry we are measuring is, at first order,

$$A_{\rm CP}(\pi\pi) = f_B A_{\rm CP}(B \to D^0/D^\star X) + (1 - f_B) A_{\rm CP}(D^0 \to \pi\pi)$$

So if both the contamination of not prompt D^0 decays, f_B, and the inclusive asymmetry $A_{\rm CP}(B \to D^0/D^\star X)$ are large the asymmetry we measure could be essentially caused by CP violation in B decays. We remove most part of not prompt decays by requiring the unsigned

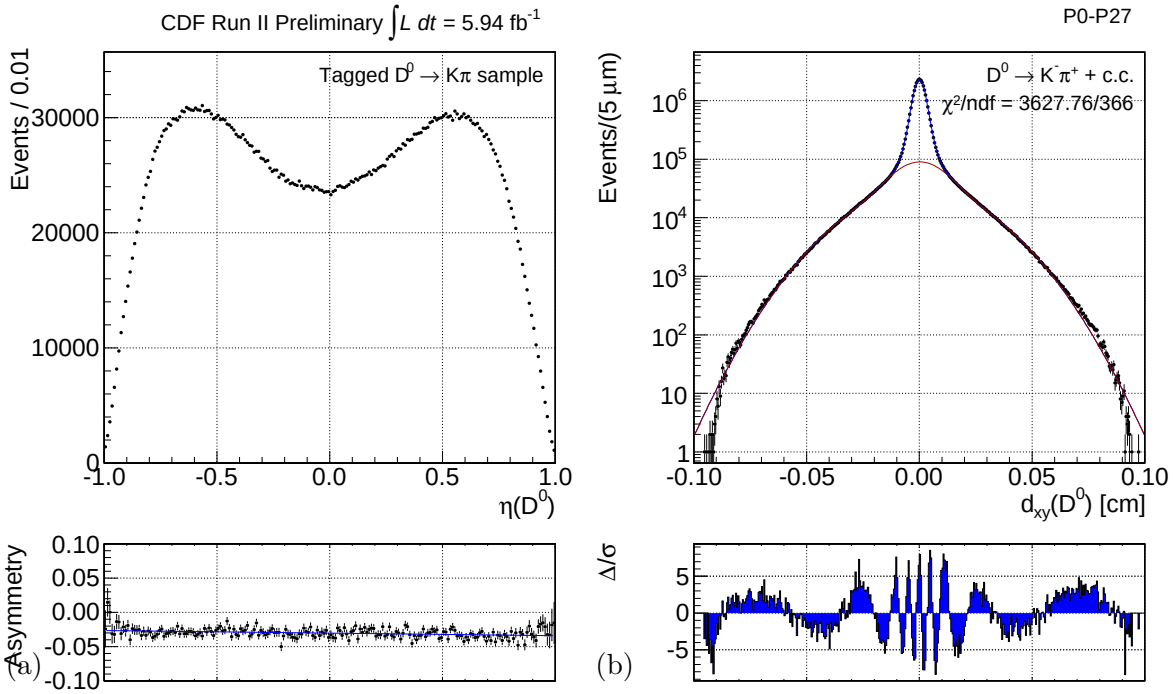

Figure 19: (a) Pseudo-rapidity distribution (top) and charge asymmetry as a function of $\eta(D^0)$ (bottom) with linear fit overlaid (blue line) of sideband subtracted tagged $D^0 \to K\pi$ decays. (b) Fit to the $d_{xy}(D^0)$ distribution of the untagged $D^0 \to K\pi$ sample.

impact parameter of the D^0 candidate not to exceed 0.01 cm. To estimate f_B we fit the $d_{xy}(D^0)$ distribution of the untagged $D^0 \to K\pi$ sample in the whole range from $[-0.1, 0.1]$ cm. We use four Gaussians to model this distribution: two for the prompt narrow peak and the other two for the not prompt broad background. Fig. 19 shows the results. A 10.3% fraction of candidates that are likely to come from B mesons decays is found. As described in [9] we evaluate the asymmetry contributed by these candidates, by repeating the untagged fit with inverted d_{xy} cut and calculating the difference with respect to the central fit that is $A_{\rm CP}(B) = (0.18 \pm 0.17)\%$ .In this worst case scenario the associated systematic uncertainty is then $f_B A_{\rm CP}(B) = 0.018\%$.

As expected we found that at the best of our knowledge, limited just by the finite size of the untagged $K\pi$ sample, there is no contribution in the measured CP violating asymmetry from non promptly produced D^0s. Practically we could repeat our measurement removing the cut on the D^0 impact parameter so to reduce the statistical resolution but, to be more conservative and since this won't be the prevalent contribution to the final systematic uncertainty, we prefer to keep the current configuration as described in this note.

6.2 Raw asymmetries extraction in the tagged samples

Since our fitting procedure is the same on both tagged samples we evaluate this kind of systematic uncertainties directly on the quantity $A_{\rm CP}^{\rm raw}(\pi\pi^\star) - A_{\rm CP}^{\rm raw}(K\pi^\star)$.

6.2.1 Shapes of fit functions

The signal shape used in the fit is extracted directly from data. To evaluate the uncertainty due to this particular choice of the analytic signal shape we repeated the fit using for the signal the parameterization extracted from MC. The results are shown in app. A.1: even if the quality of the fit is unsatisfactory we observe only a small difference on the measured asymmetries, which gives a variation on the tagged raw asymmetries difference of 0.006%.

The background shape parameters are floating in the fits. Assuming, as done for signal, that the background shape of $D^0 \to K\pi$ tagged decays is the same as in $D^0 \to \pi\pi$ decays we fix the background shape in the $D^0 \to \pi\pi$ fit to the one obtained in the fit to the higher statistic $D^0 \to K\pi$ sample. The observed variation on the result is 0.003%.

The systematic uncertainty associated to the templates used in the fit is then evaluated as the sum in quadrature: $\Delta[A_{\rm CP}^{\rm raw}(\pi\pi^\star) - A_{\rm CP}^{\rm raw}(K\pi^\star)] = 0.007\%$.

6.2.2 Charge-dependent mass resolution

We observed small differences between $M(D^0\pi_s)$ distributions of positive and negative $D^\star$ candidates selected in their $D^0(\to K\pi)\pi$ decay. This is somewhat plausible because of possible tiny differences in tracking resolutions between positive and negative tracks at low momentum. However, this is potentially dangerous for our measurement because it impacts at first order in the observed asymmetry. To evaluate an associated systematic uncertainty we repeated the fit after fixing signal shapes to be the same and/or leaving background shapes to vary independently for positive and negative $D^\star$ candidates. The values of the shape parameters in the $D^0 \to \pi\pi$ fit are always fixed to the ones obtained on the $D^0 \to K\pi$ sample. All results are shown in app. A.2 and summarized in tab. 5: the maximum observed variation (i.e. the worst case) is 0.088%, which occurs when both background shapes' parameters vary independently for positive and negative samples while δ_J is combined.

6.2.3 Residual physics backgrounds

A further source of systematic uncertainty could be imperfect subtraction of physics backgrounds. Our tagged samples are selected by requiring the D^0 mass within 24 MeV/c^2 from the known value. We estimated with simulation that a $\sim 0.22\%$ (tagged $\pi\pi$ sample) and $\sim 0.77\%$ (tagged $K\pi$) contamination from physics backgrounds survives this selection. The contamination in the $\pi\pi$ sample is essentially due to the high mass tail of the $D^0 \to K\pi$ peak

Case	χ^2/ndf		Variation (%) on
	$K\pi^\star$	$\pi\pi^\star$	$A_{\rm CP}^{\rm raw}(\pi\pi^\star) - A_{\rm CP}^{\rm raw}(K\pi^\star)$
δ_J, b, c combined	414/306	301/306	0.019
δ_J, b combined, c free	397/305	327/307	0.072
δ_J, c combined, b free	401/305	331/307	0.048
δ_J combined, b, c free	396/304	332/308	0.088
b combined, δ_J, c free	384/303	323/307	0.020
c combined, δ_J, b free	384/303	328/307	0.015
δ_J, b, c free	383/302	328/308	0.012

Table 5: Variation on the fit results with respect to the central fit with different input conditions.

while the tagged $K\pi$ sample is affected by a tail from partially reconstructed D^0 decays. The asymmetry as a function of the D^0 mass, fig. 20, shows that no large differences arise in observed asymmetry between our signal and background regions. We use the fitted value of $A_{\rm CP}^{\rm raw}(K\pi^\star)$ as possible asymmetry induced by imperfect subtraction of background in the tagged $D^0 \to \pi\pi$ sample. For the tagged $D^0 \to K\pi$ sample we evaluate the background asymmetry by fitting the asymmetry plot in fig. 20 (b) in the region $M(K\pi) < 1.8$ GeV/c^2. The maximum bias in the fitted raw asymmetries difference is then given by

$$\Delta[A_{\rm CP}^{\rm raw}(\pi\pi^\star) - A_{\rm CP}^{\rm raw}(K\pi^\star)] = 0.22\% \, [A_{\rm CP}^{\rm raw}(\pi\pi^\star) - A_{\rm CP}^{\rm raw}(K\pi^\star)] \\ - 0.77\% \, [A_{\rm CP}^{\rm raw}(K\pi^\star) - A_{\rm CP}^{\rm raw}(M(K\pi) < 1.8)] = 0.005\%$$

6.2.4 Imperfect reweighing

To calculate reweighing functions we compared distributions of pure signals obtained by means of sideband-subtraction. A systematic uncertainty arise from any imperfection in this procedure. To evaluate an upper limit on the size of this systematic uncertainty we re-calculated the reweighing functions without applying any sideband subtraction and we repeated the fit on the tagged $D^0 \to \pi\pi$ sample. We found a variation in the raw asymmetry of $\Delta A_{\rm CP}^{\rm raw}(\pi\pi^\star) = 0.0001\%$, negligible with respect to the other systematic uncertainties.

6.3 Summary

Tab. 6 summarizes the set of systematic uncertainties considered in our measurement (the systematic uncertainties on the extraction of the raw asymmetry in the untagged sample are described in [9]). Assuming they are independent and summing in quadrature we obtain a total systematic uncertainty on our final $A_{\rm CP}(\pi\pi)$ measurement of 0.10%. This achievement,

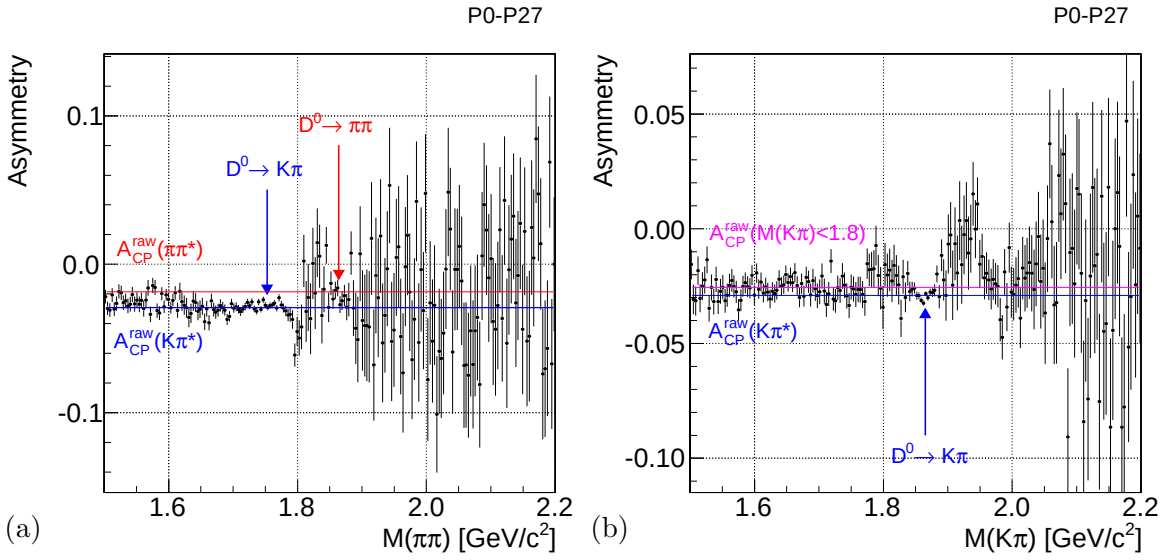

Figure 20: Asymmetry as a function of $M(\pi\pi)$ (a) and $M(K\pi)$ (b) for tagged D^0 decays. The plots also show the asymmetry level of signals and backgrounds in both samples, the difference between these two values is used to set an upper limit to the systematic uncertainty that comes from not subtracted backgrounds in the two tagged samples.

not so obvious in flavor-physics measurement in hadron collisions, meets our initial goal of suppressing the size of systematic uncertainties below the statistical ones.

Source of systematic uncertainty	Variation (%) on		
	$A_{\rm CP}^{\rm raw}(\pi\pi^\star) - A_{\rm CP}^{\rm raw}(K\pi^\star)$	$A_{\rm CP}^{\rm raw}(K\pi)$	$A_{\rm CP}(\pi\pi)$
Reliability of our cancellation	–	–	0.010
Beam drag effects	–	–	0.004
Contamination of not prompt D^0s	–	–	0.018
Templates used in fits	0.007	0.005	–
Templates charge differences	0.088	0.044	–
Asymmetries from physical backgrounds	0.005	0.011	–
Samples reweighting	0.0001	0.0005	–
Subtotal	0.088	0.046	0.021
Total	–	–	0.101

Table 6: Summary of systematic uncertainties. The subtotal is the sum in quadrature of the corresponding column, the total is the sum in quadrature of all uncertainties.

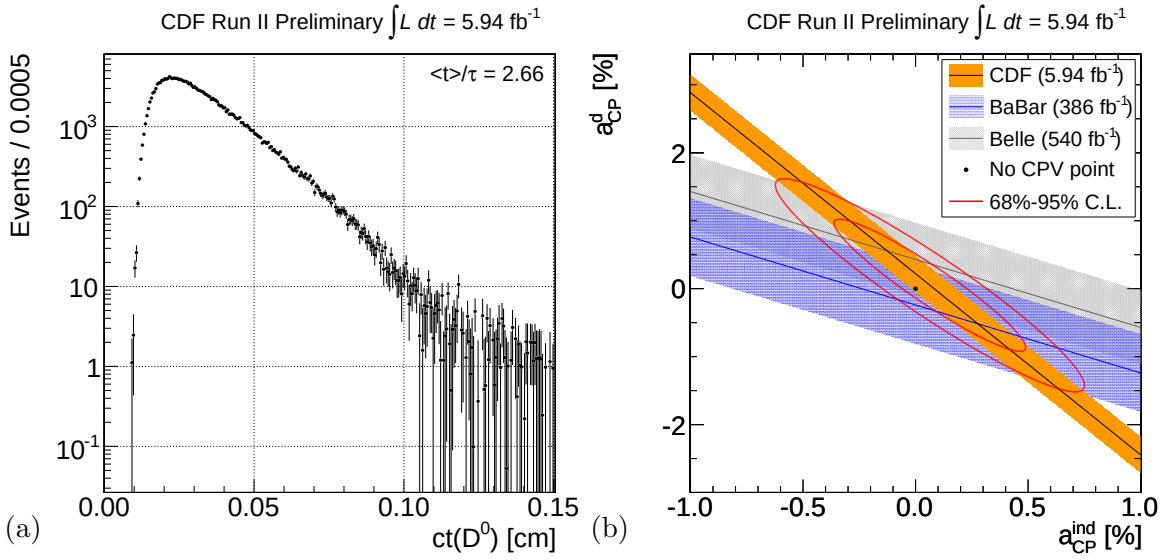

Figure 21: Proper decay lenght distribution of sideband-subtracted tagged $D^0 \to \pi\pi$ data (a). Combination of our measuremetn with current best results from B-factories in the parameter space $(a_{\rm CP}^{\rm ind}, a_{\rm CP}^{\rm dir})$ (b).

7 Final result and conclusions

We reported the measurement of time-integrated CP violating asymmetry in $D^0 \to \pi^+\pi^-$ decays using 5.94 fb^{-1} of Two Track Trigger data. The final result is

$$A_{\rm CP}(D^0 \to \pi^+\pi^-) = \left[+0.22 \pm 0.24\ (stat.) \pm 0.10\ (syst.)\right]\%,$$

which is consistent with CP conservation and also with the SM predictions.

To disentangle the independent contributions of direct and indirect CP violation in $D^0 \to \pi^+\pi^-$ decays an analysis where the time evolution of charm decays is fitted is needed. Nevertheless some interesting conclusions could be derived either comparing our result with B-factories measurements or making some theoretical assumptions.

As stated in eq. (3), the measured integrated CP asymmetry is at first order the linear combination of a direct, $a_{\rm CP}^{\rm dir}$, and an indirect, $a_{\rm CP}^{\rm ind}$, CP violating asimmetry through a coefficient that is the mean proper decay time of D^0 candidates in the data sample. Fig. 21 (a) shows that our tagged $D^0 \to \pi^+\pi^-$ sample has a mean proper decay time that is 2.66 times the D^0 lifetime. This means that our measurement describes a straight band in the plane $(a_{\rm CP}^{\rm ind}, a_{\rm CP}^{\rm dir})$ with angular coefficient -2.66. The same holds for B-factories' measurements, with angular coefficient -1 [2], due to their reduced acceptance in charm decay time. Combination of the three measurements allows construction of confidence intervals on both $a_{\rm CP}^{\rm ind}$ and $a_{\rm CP}^{\rm dir}$. Fig. 21 (b) shows the combination assuming Gaussian uncertainties: the bands are 1σ wide and the red curves represent the 68% and 95% CL limits of the combined result.

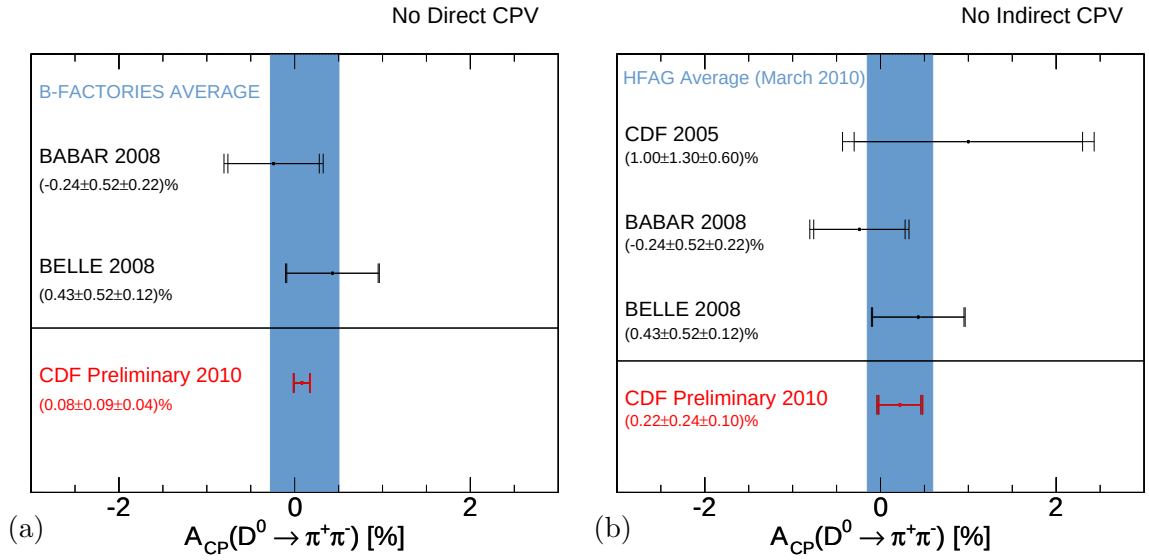

Figure 22: Comparison of our measurement with B-factories ones assuming that no direct (a) or indirect (b) CP violation can occur.

An even more interesting result could be obtained if we assume no direct CP violation with rather good approximation in the charm sector, as SM expectations suggest [1]. In this case eq. (3) simplifies to

$$A_{\rm CP}(\pi^+\pi^-) \approx \frac{\langle t \rangle}{\tau} a_{\rm CP}^{\rm ind}$$

so

$$a_{\rm CP}^{\rm ind} = \left[+0.08 \pm 0.09 \ (stat.) \pm 0.04 \ (syst.) \right].$$

This measurement would then imply that the range $[-0.109, 0.274]\%$ covers $a_{\rm CP}^{\rm ind}$ at the 95% CL. Note that, since $\langle t \rangle / \tau$ in our sample is greater than in B-factories ones, this range is more than five times tighter than the ones obtained using B-factories measurements, as shown in fig. 22 (a).

If, on the contrary, we assume CP conservation in $D^0 - \overline{D}^0$ mixing, our number is directly comparable to other measurements in different experimental configurations. In this case, fig. 22 (b), our statistical uncertainties are half those from the best B-factories measurements, and also systematic uncertainties are smaller.

References

[1] "CP violation for neutral charmed meson decays into CP eigenstates", *Eur. Phys. J.* **C 50** (2007) 579.

[2] Most recent B-factories measurements: *Phys. Rev. Lett.* **100** (2008) 061803, *Phys. Lett.* **B 670** (2008) 190.

[3] Published CDF measurement: *Phys. Rev. Lett.* **94** (2005) 122001.

[4] "A Method to Suppress Detector Asymmetries in the Measurement of $A_{\rm CP}$ in $D^0 \to \pi^+\pi^-$ and $D^0 \to K^+K^-$", CDF Note 10132.

[5] B-MC webpage.

[6] BStNtuples Twiki Page.

[7] "Measurement of the efficiency ratio $\epsilon(K^-\pi^+)/\epsilon(K^+\pi^-)$ from $D^0 \to K^-\pi^+$ decays", CDF Note 8463.

[8] "Trigger composition for the analysis of $D^0 \to h^+h'^-$ decays", CDF Note 10236.

[9] "Uncorrected Charge Asymmetry in the Untagged $D^0 \to K^-\pi^+$ Decays", CDF Note 10214

A Appendix

A.1 B-MC template for signals

$D^0 \to K\pi$ fit

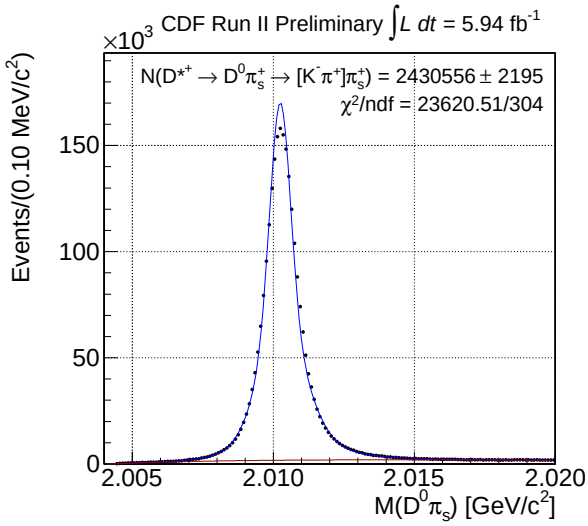

(a)

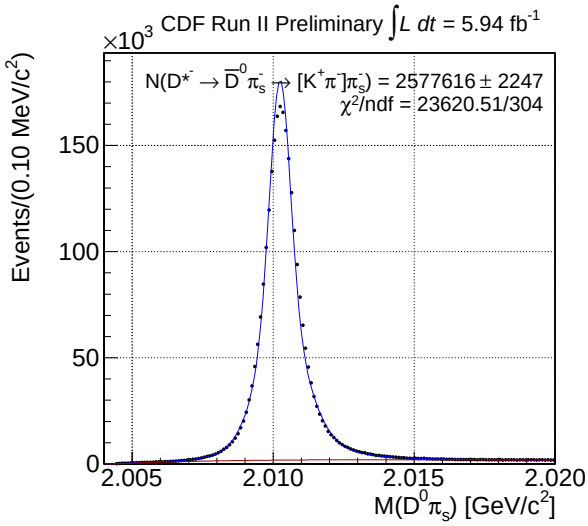

(b)

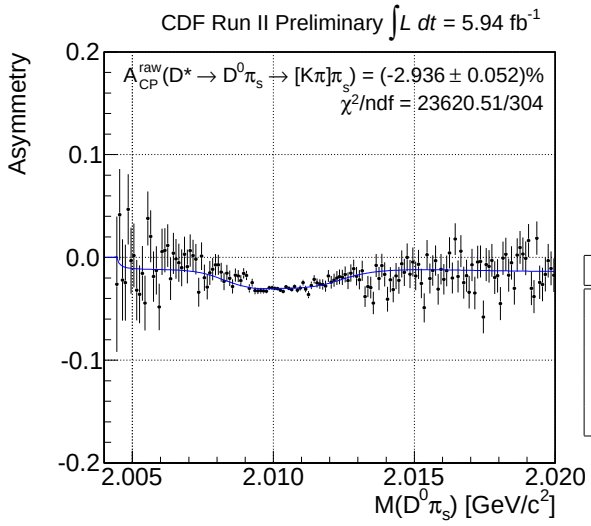

(c)

(d)

PAR	POS VALUE	NEG VALUE	ASYMMETRY
$N_{\rm sgn}$	2430556 ± 2195	2577616 ± 2247	$(-2.936 \pm 0.052)\%$
δ_J	1.247 ± 0.003	1.260 ± 0.003	$(-5.08 \pm 1.46) \times 10^{-3}$
$N_{\rm bkg}$	246242 ± 1619	253459 ± 1640	$(-1.44 \pm 0.29)\%$
b	0.90 ± 0.01	combined	
c	93 ± 2	combined	

$D^0 \to \pi\pi$ **fit**

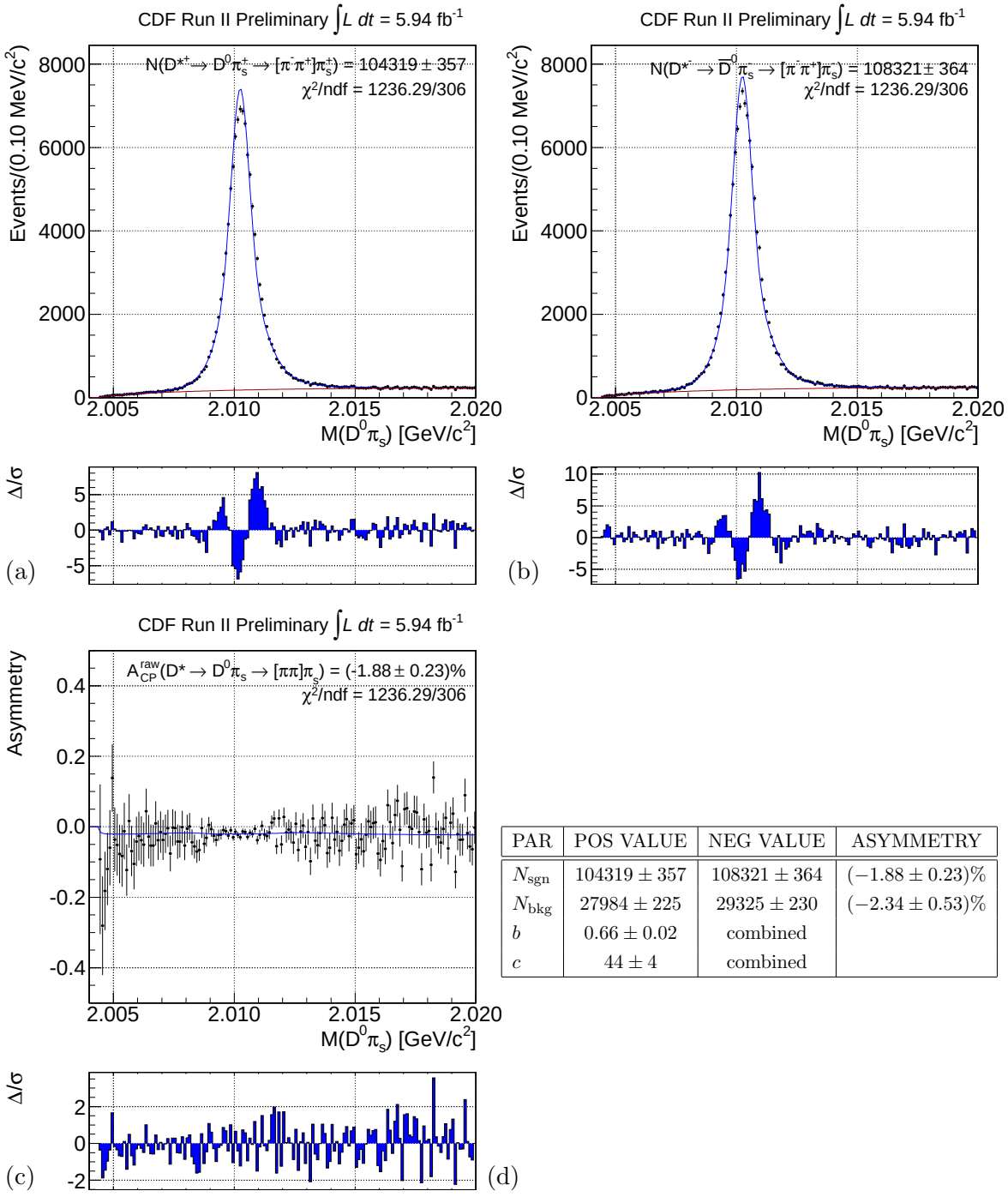

PAR	POS VALUE	NEG VALUE	ASYMMETRY
$N_{\rm sgn}$	104319 ± 357	108321 ± 364	$(-1.88 \pm 0.23)\%$
$N_{\rm bkg}$	27984 ± 225	29325 ± 230	$(-2.34 \pm 0.53)\%$
b	0.66 ± 0.02	combined	
c	44 ± 4	combined	

A.2 Differencies between positive and negative signal shapes

A.2.1 Case $\delta_J,\ b,\ c$ combined

$D^0 \to K\pi$ fit

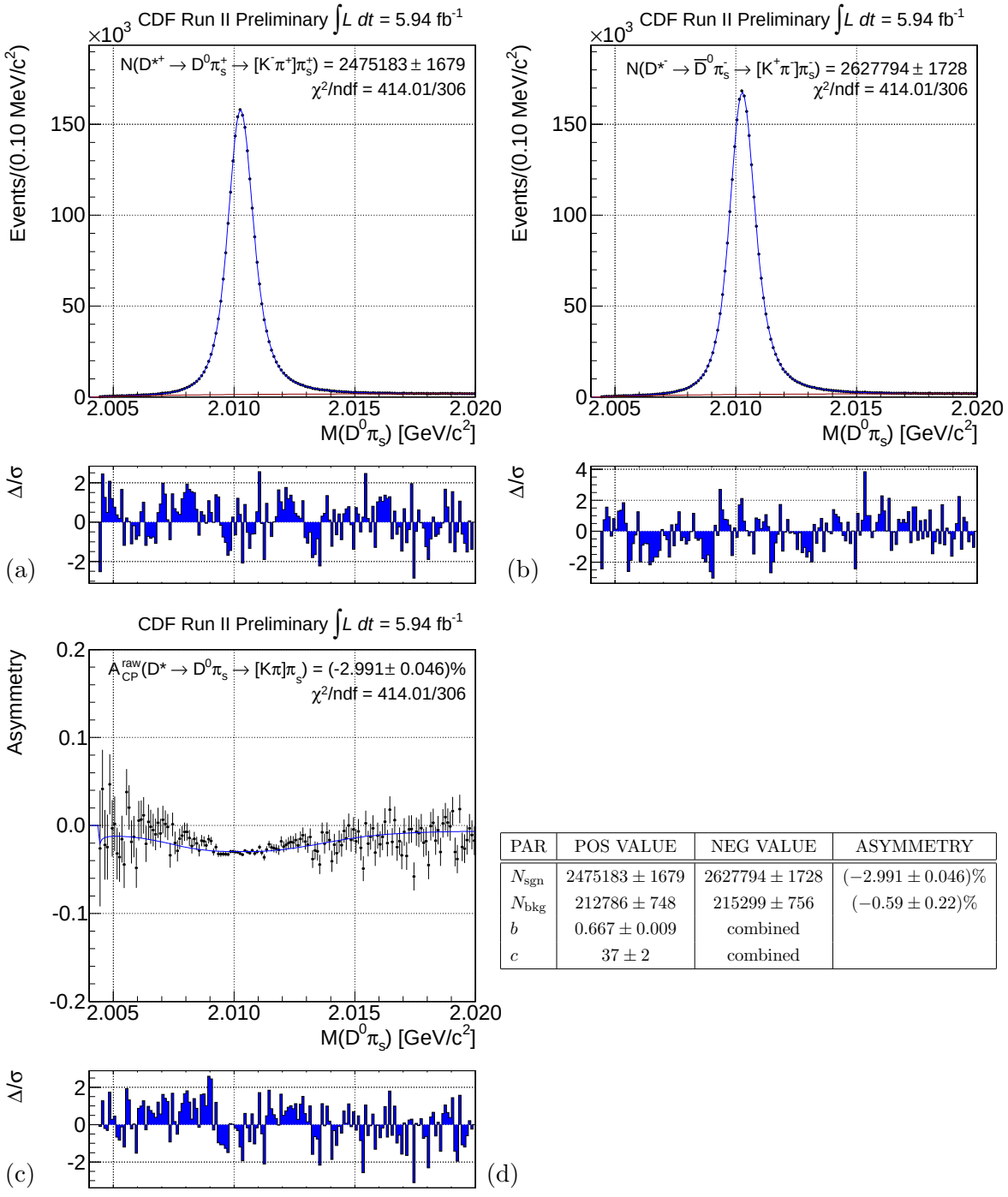

PAR	POS VALUE	NEG VALUE	ASYMMETRY
$N_{\rm sgn}$	2475183 ± 1679	2627794 ± 1728	$(-2.991 \pm 0.046)\%$
$N_{\rm bkg}$	212786 ± 748	215299 ± 756	$(-0.59 \pm 0.22)\%$
b	0.667 ± 0.009	combined	
c	37 ± 2	combined	

$D^0 \to \pi\pi$ **fit**

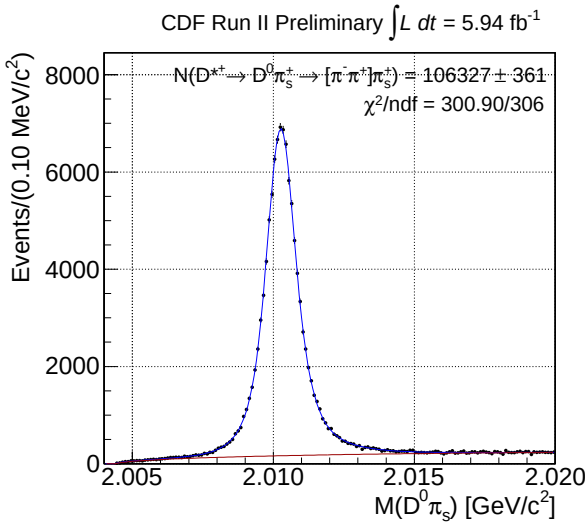

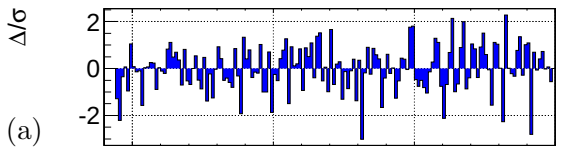

(a)

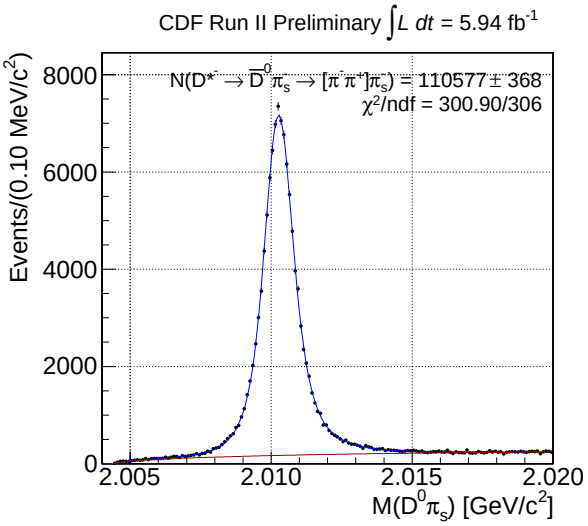

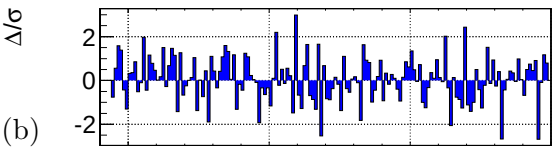

(b)

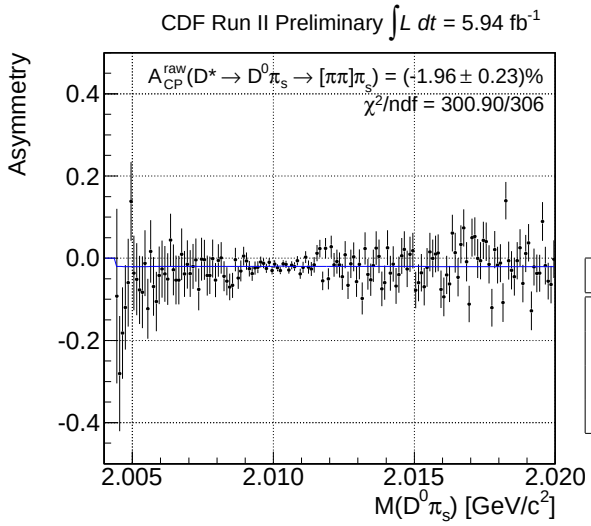

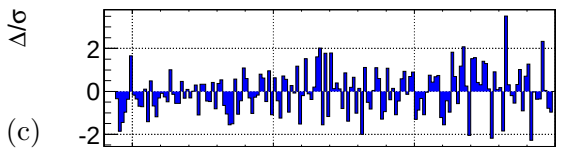

(c)

(d)

PAR	POS VALUE	NEG VALUE	ASYMMETRY
$N_{\rm sgn}$	106327 ± 361	110577 ± 368	$(-1.96 \pm 0.23)\%$
$N_{\rm bkg}$	26448 ± 223	27546 ± 228	$(-2.03 \pm 0.54)\%$
b	0.57 ± 0.02	combined	
c	22 ± 4	combined	

A.2.2 Case δ_J, b combined, c free

$D^0 \to K\pi$ fit

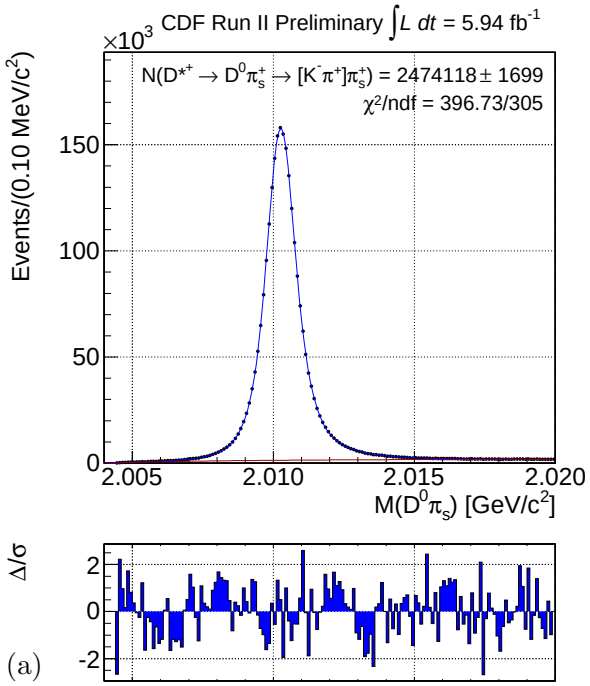

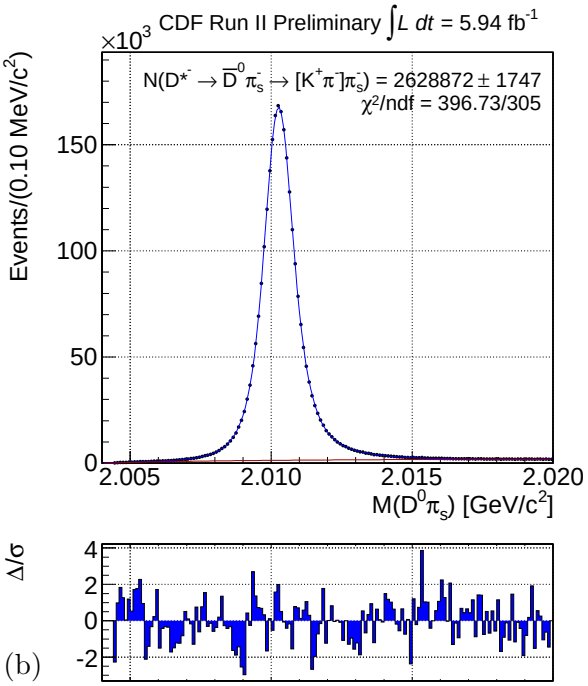

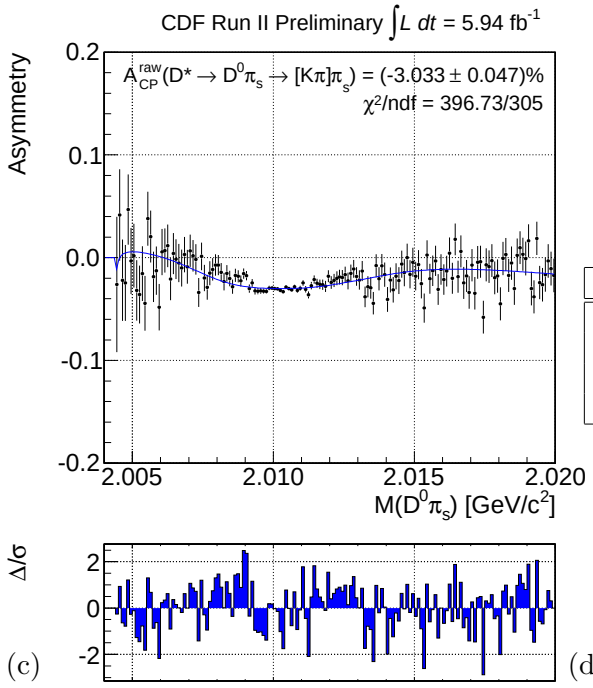

(d)

PAR	POS VALUE	NEG VALUE	ASYMMETRY
$N_{\rm sgn}$	2474118 ± 1699	2628872 ± 1747	$(-3.033 \pm 0.047)\%$
$N_{\rm bkg}$	213861 ± 792	214232 ± 798	$(-0.9 \pm 2.5) \times 10^{-3}$
b	0.667 ± 0.009	combined	
c	39 ± 2	34 ± 2	$(6.2 \pm 1.5)\%$

$D^0 \to \pi\pi$ **fit**

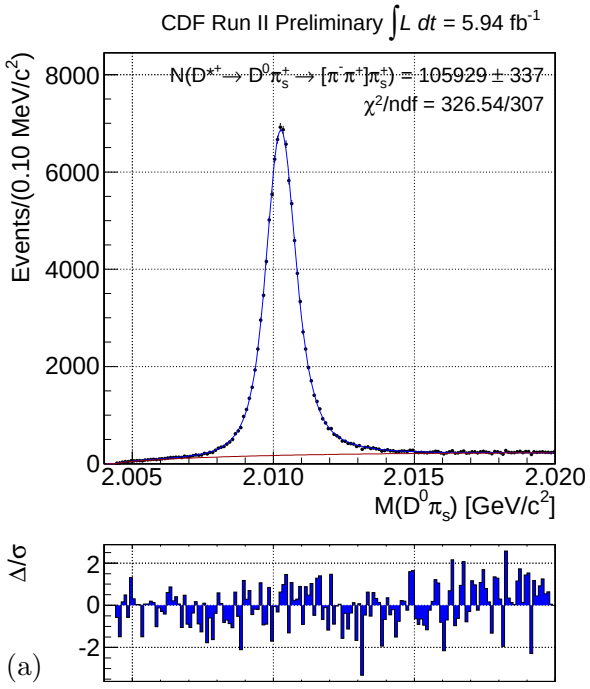

(a)

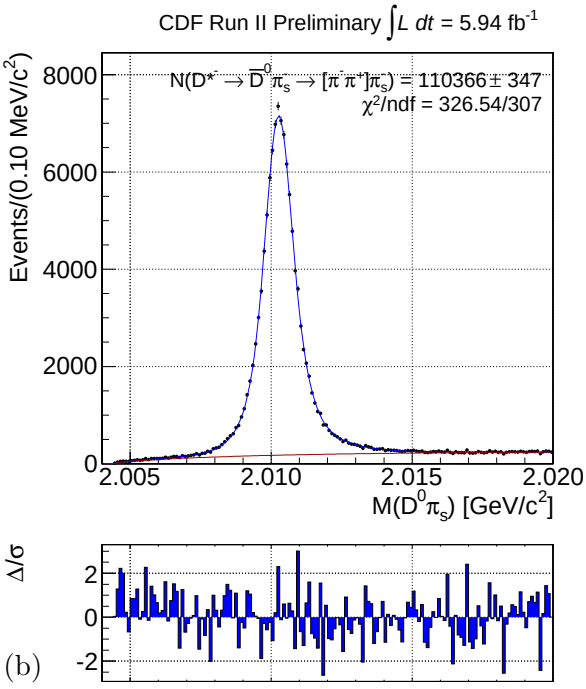

(b)

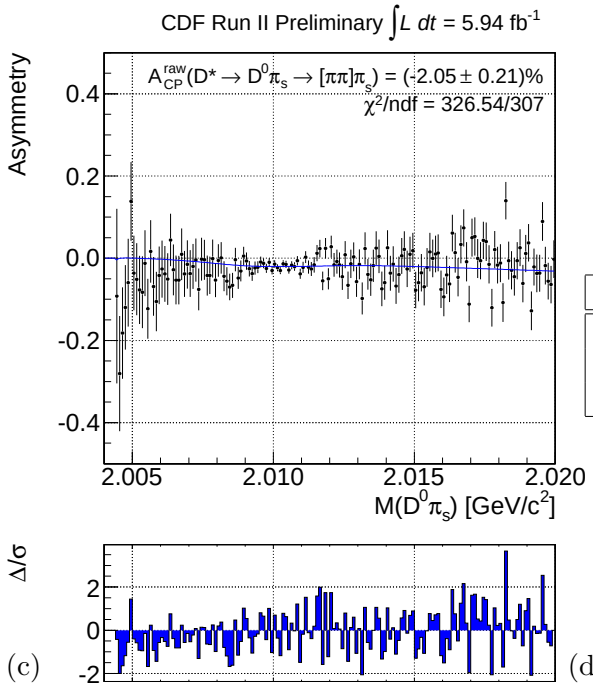

(c)

(d)

PAR	POS VALUE	NEG VALUE	ASYMMETRY
$N_{\rm sgn}$	105929 ± 337	110366 ± 347	$(-2.05 \pm 0.21)\%$
$N_{\rm bkg}$	26832 ± 207	27746 ± 207	$(-1.67 \pm 0.51)\%$
b	0.649 ± 0.008	combined	

A.2.3 Case δ_J, c combined, b free

$D^0 \to K\pi$ **fit**

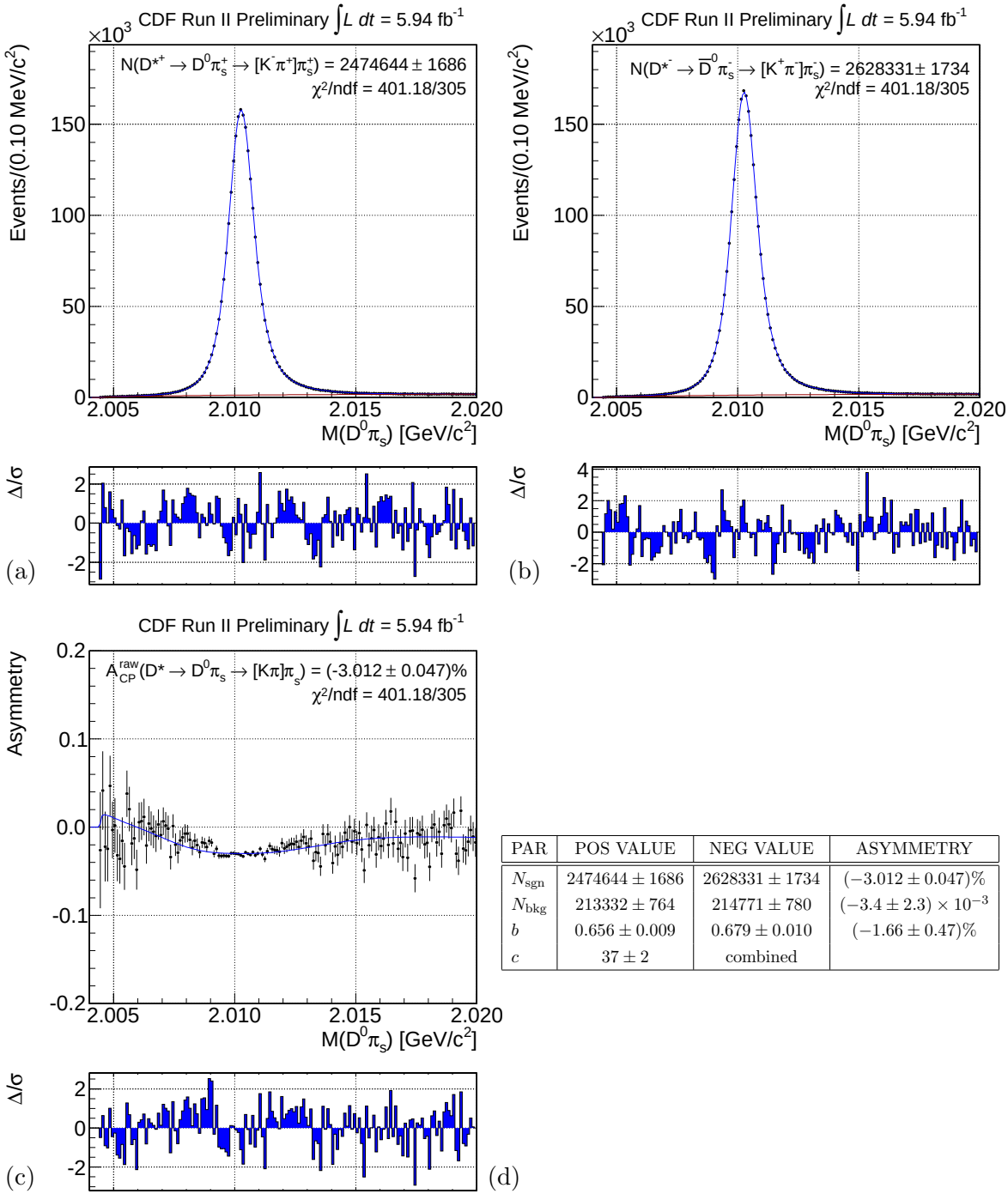

PAR	POS VALUE	NEG VALUE	ASYMMETRY
$N_{\rm sgn}$	2474644 ± 1686	2628331 ± 1734	$(-3.012 \pm 0.047)\%$
$N_{\rm bkg}$	213332 ± 764	214771 ± 780	$(-3.4 \pm 2.3) \times 10^{-3}$
b	0.656 ± 0.009	0.679 ± 0.010	$(-1.66 \pm 0.47)\%$
c	37 ± 2	combined	

$D^0 \to \pi\pi$ **fit**

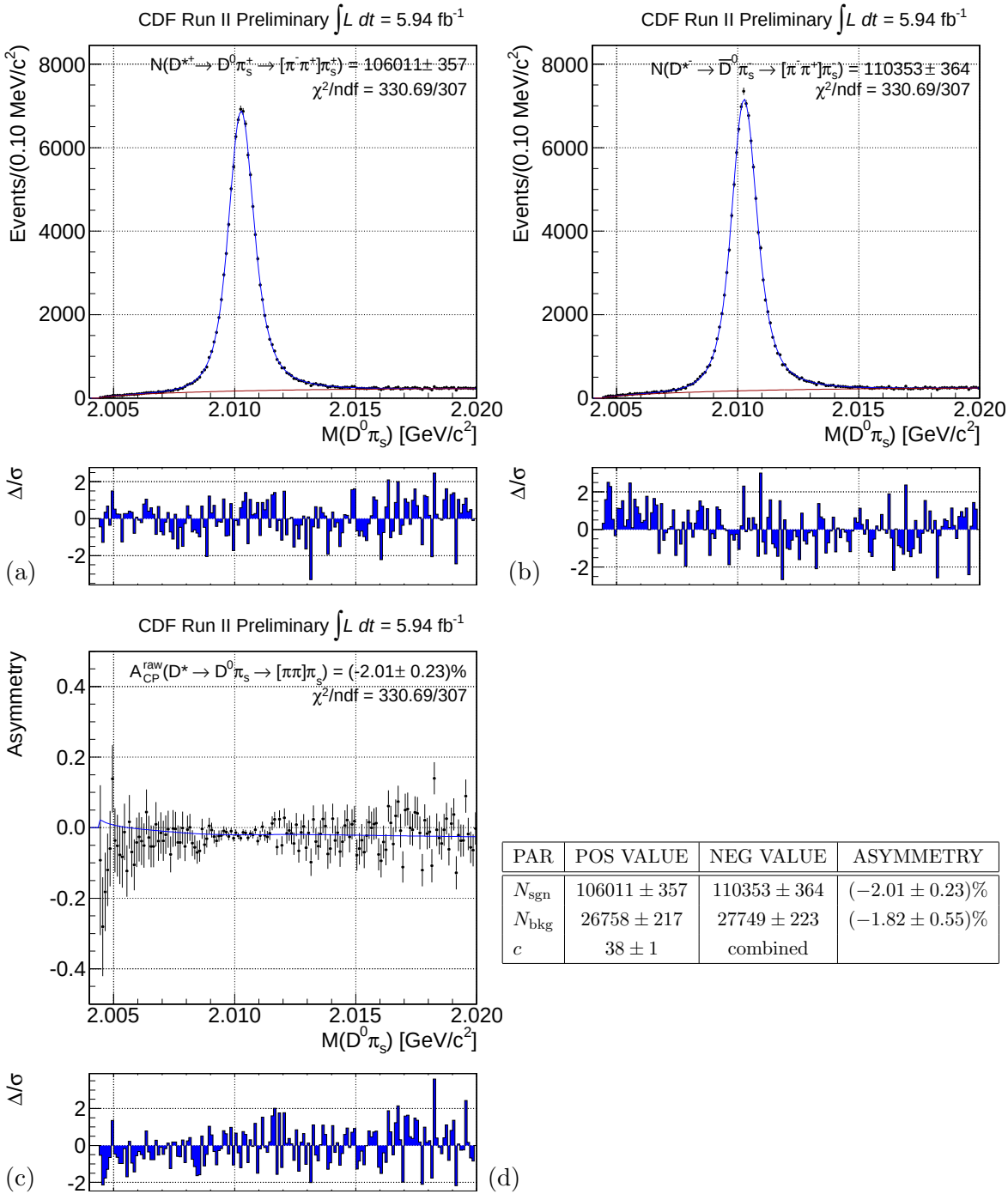

PAR	POS VALUE	NEG VALUE	ASYMMETRY
$N_{\rm sgn}$	106011 ± 357	110353 ± 364	$(-2.01 \pm 0.23)\%$
$N_{\rm bkg}$	26758 ± 217	27749 ± 223	$(-1.82 \pm 0.55)\%$
c	38 ± 1	combined	

A.2.4 Case δ_J combined, b, c free

$D^0 \to K\pi$ **fit**

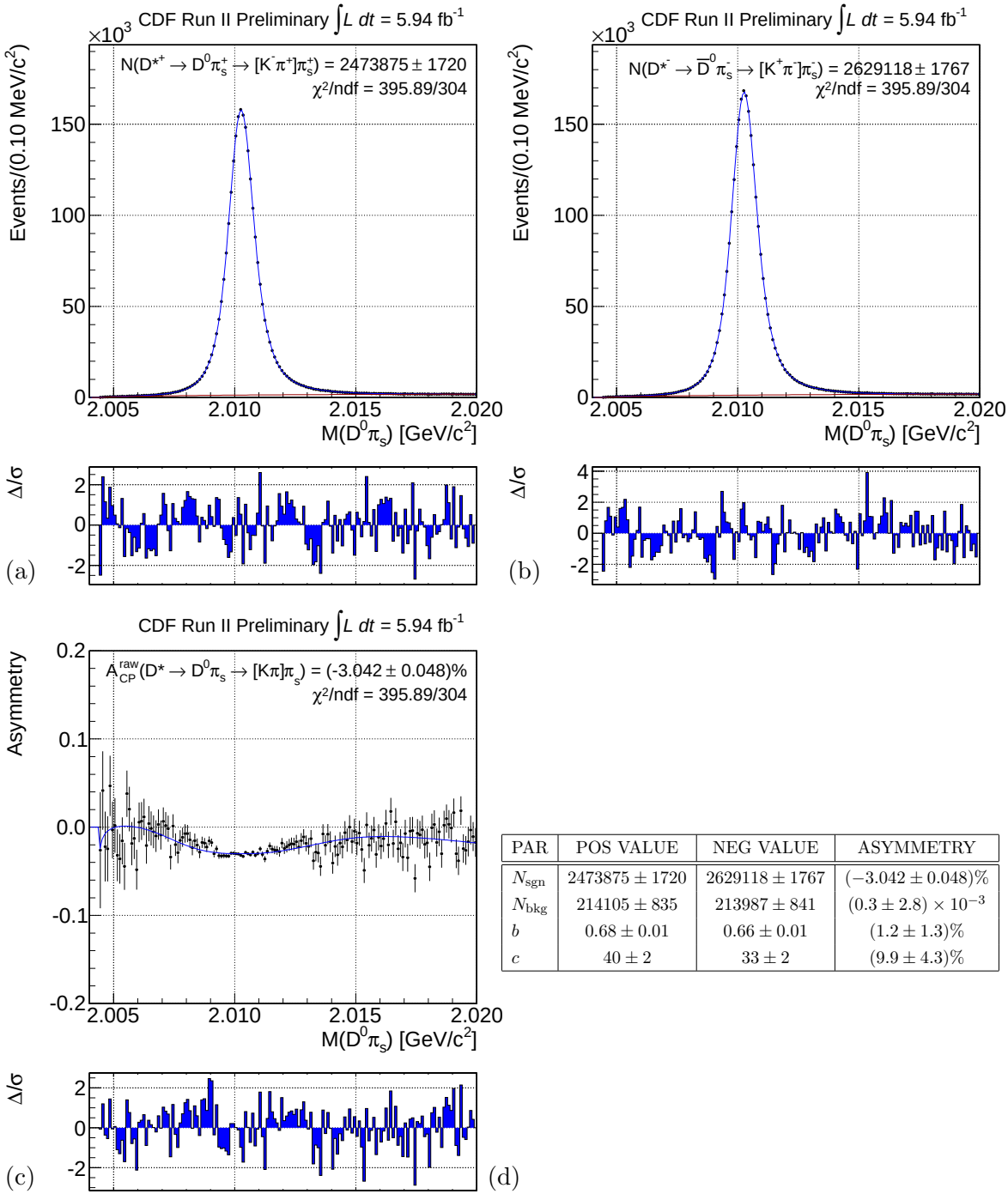

PAR	POS VALUE	NEG VALUE	ASYMMETRY
$N_{\rm sgn}$	2473875 ± 1720	2629118 ± 1767	$(-3.042 \pm 0.048)\%$
$N_{\rm bkg}$	214105 ± 835	213987 ± 841	$(0.3 \pm 2.8) \times 10^{-3}$
b	0.68 ± 0.01	0.66 ± 0.01	$(1.2 \pm 1.3)\%$
c	40 ± 2	33 ± 2	$(9.9 \pm 4.3)\%$

$D^0 \to \pi\pi$ **fit**

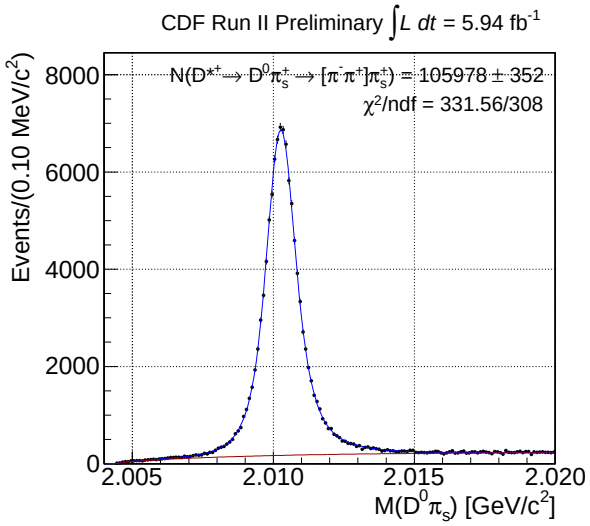

(a)

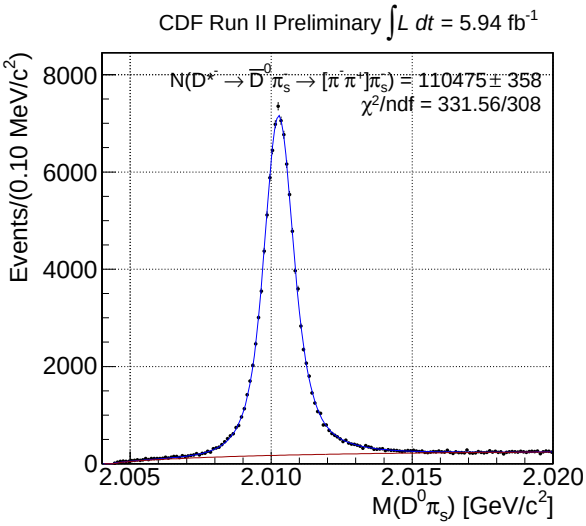

(b)

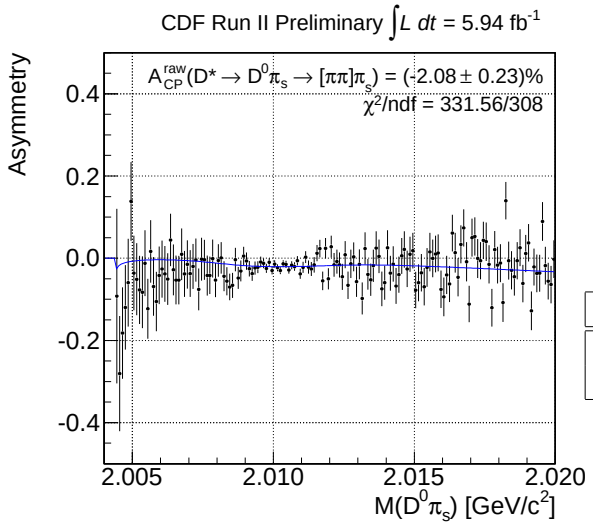

(c)

(d)

PAR	POS VALUE	NEG VALUE	ASYMMETRY
$N_{\rm sgn}$	105978 ± 352	110475 ± 358	$(-2.08 \pm 0.23)\%$
$N_{\rm bkg}$	26789 ± 210	27628 ± 212	$(-1.54 \pm 0.55)\%$

A.2.5 Case b combined, δ_J, c free

$D^0 \to K\pi$ **fit**

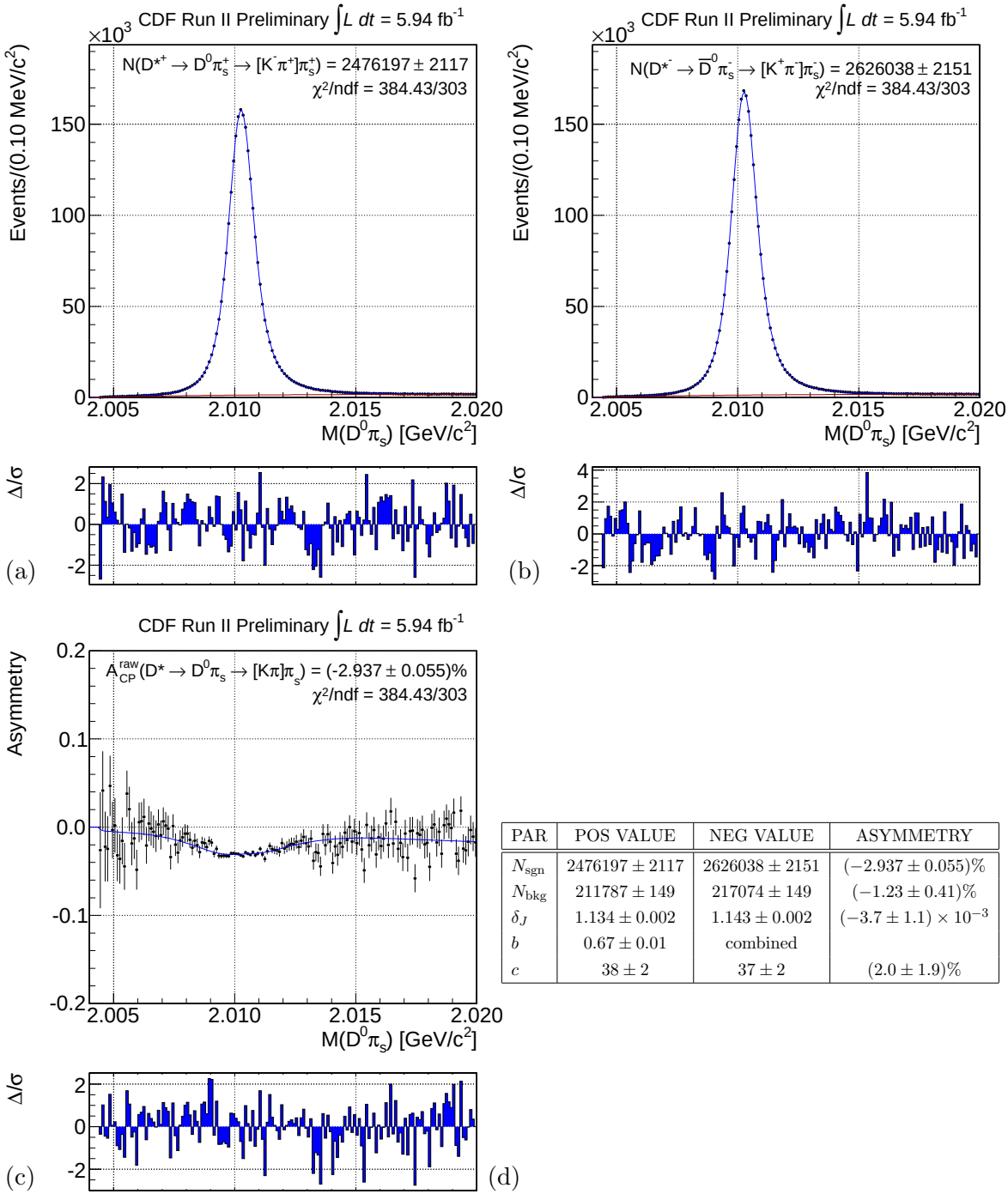

PAR	POS VALUE	NEG VALUE	ASYMMETRY
$N_{\rm sgn}$	2476197 ± 2117	2626038 ± 2151	$(-2.937 \pm 0.055)\%$
$N_{\rm bkg}$	211787 ± 149	217074 ± 149	$(-1.23 \pm 0.41)\%$
δ_J	1.134 ± 0.002	1.143 ± 0.002	$(-3.7 \pm 1.1) \times 10^{-3}$
b	0.67 ± 0.01	combined	
c	38 ± 2	37 ± 2	$(2.0 \pm 1.9)\%$

$D^0 \to \pi\pi$ **fit**

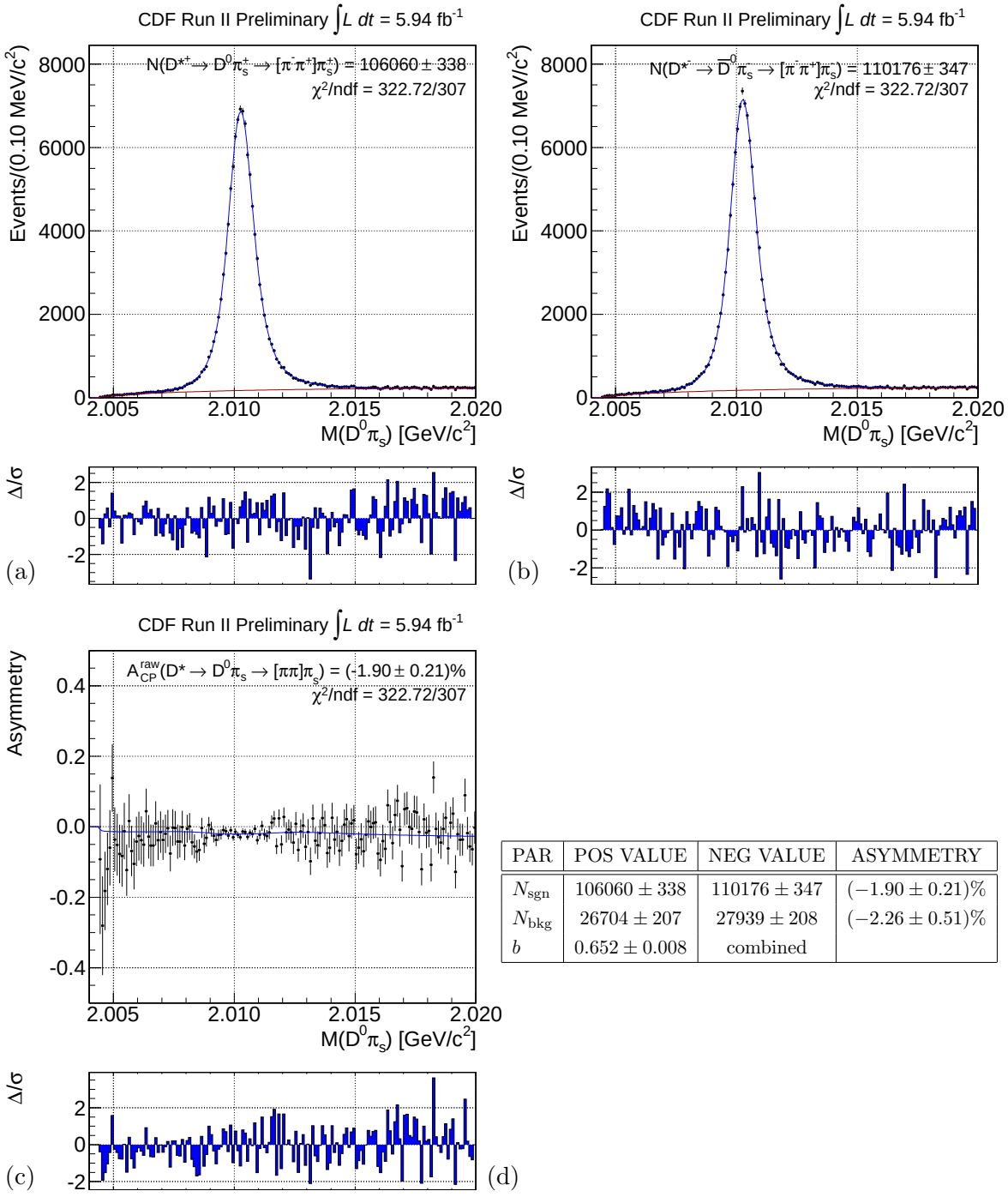

PAR	POS VALUE	NEG VALUE	ASYMMETRY
$N_{\rm sgn}$	106060 ± 338	110176 ± 347	$(-1.90 \pm 0.21)\%$
$N_{\rm bkg}$	26704 ± 207	27939 ± 208	$(-2.26 \pm 0.51)\%$
b	0.652 ± 0.008	combined	

A.2.6 Case c combined, δ_J, b free

$D^0 \to K\pi$ fit

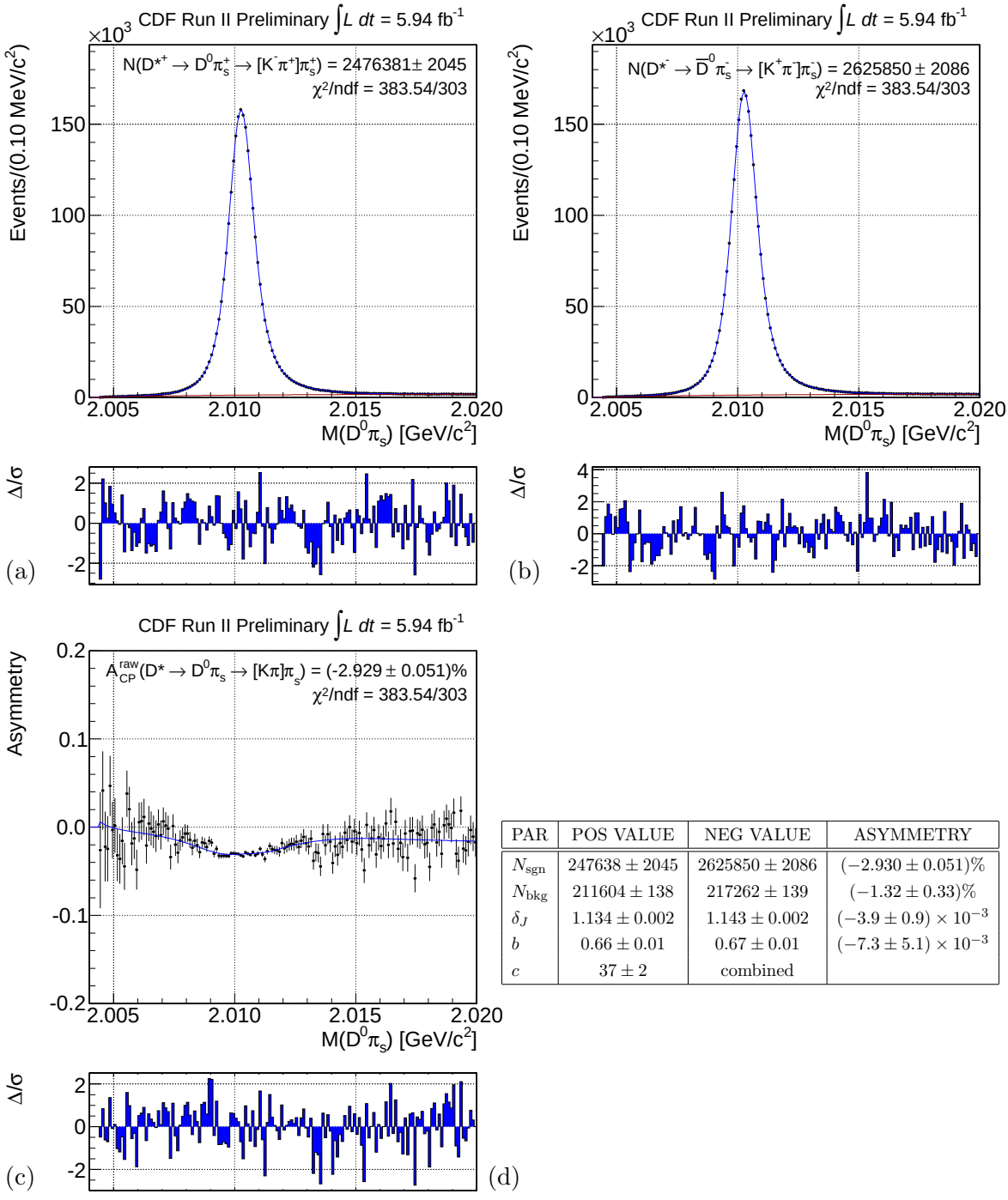

PAR	POS VALUE	NEG VALUE	ASYMMETRY
$N_{\rm sgn}$	247638 ± 2045	2625850 ± 2086	$(-2.930 \pm 0.051)\%$
$N_{\rm bkg}$	211604 ± 138	217262 ± 139	$(-1.32 \pm 0.33)\%$
δ_J	1.134 ± 0.002	1.143 ± 0.002	$(-3.9 \pm 0.9) \times 10^{-3}$
b	0.66 ± 0.01	0.67 ± 0.01	$(-7.3 \pm 5.1) \times 10^{-3}$
c	37 ± 2	combined	

$D^0 \to \pi\pi$ **fit**

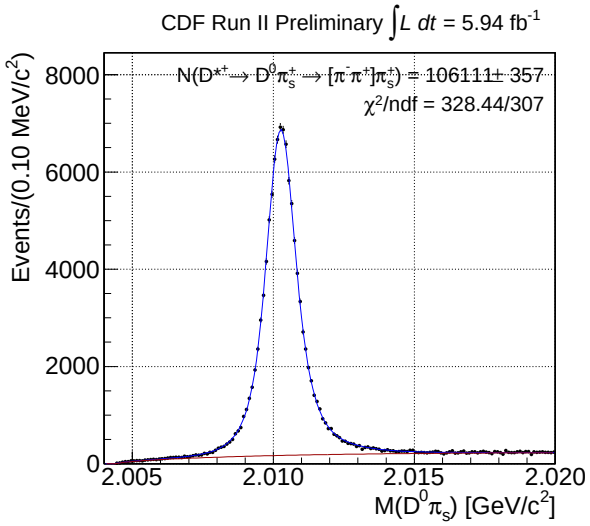

(a)

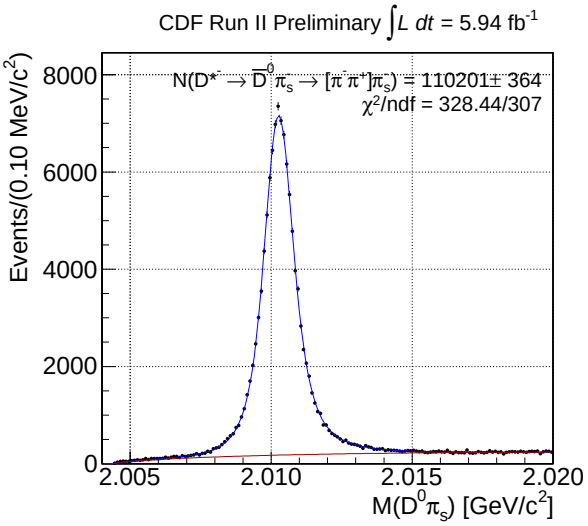

(b)

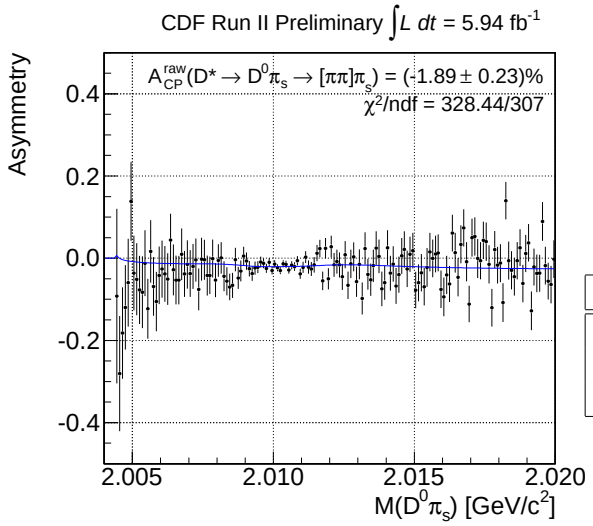

(c)

(d)

PAR	POS VALUE	NEG VALUE	ASYMMETRY
$N_{\rm sgn}$	106111 ± 357	110201 ± 364	$(-1.89 \pm 0.23)\%$
$N_{\rm bkg}$	26656 ± 217	27904 ± 223	$(-2.29 \pm 0.55)\%$
c	38 ± 1	combined	

A.2.7 Case δ_J, b, c free

$D^0 \to K\pi$ **fit**

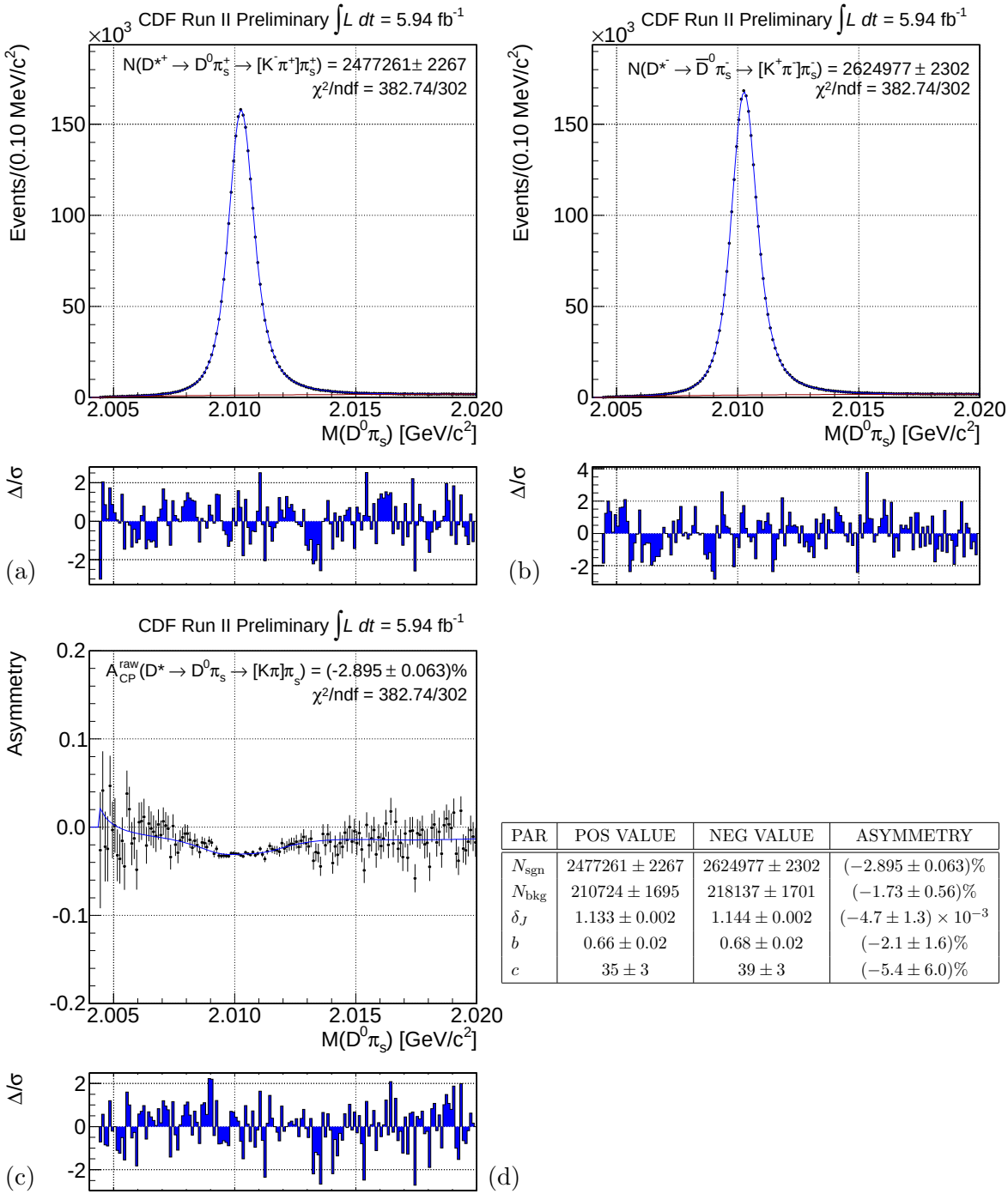

PAR	POS VALUE	NEG VALUE	ASYMMETRY
$N_{\rm sgn}$	2477261 ± 2267	2624977 ± 2302	$(-2.895 \pm 0.063)\%$
$N_{\rm bkg}$	210724 ± 1695	218137 ± 1701	$(-1.73 \pm 0.56)\%$
δ_J	1.133 ± 0.002	1.144 ± 0.002	$(-4.7 \pm 1.3) \times 10^{-3}$
b	0.66 ± 0.02	0.68 ± 0.02	$(-2.1 \pm 1.6)\%$
c	35 ± 3	39 ± 3	$(-5.4 \pm 6.0)\%$

$D^0 \to \pi\pi$ **fit**

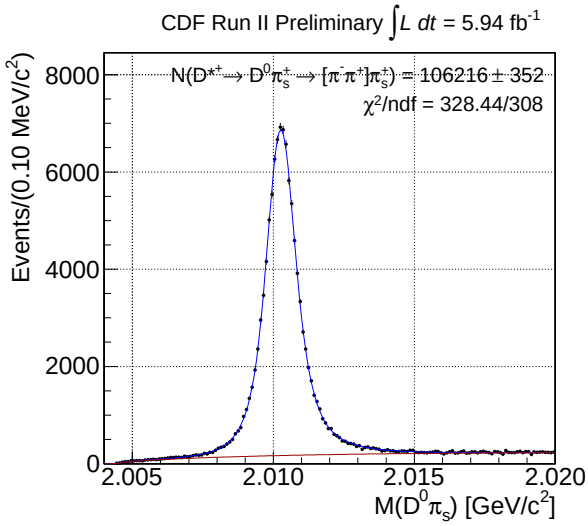

(a)

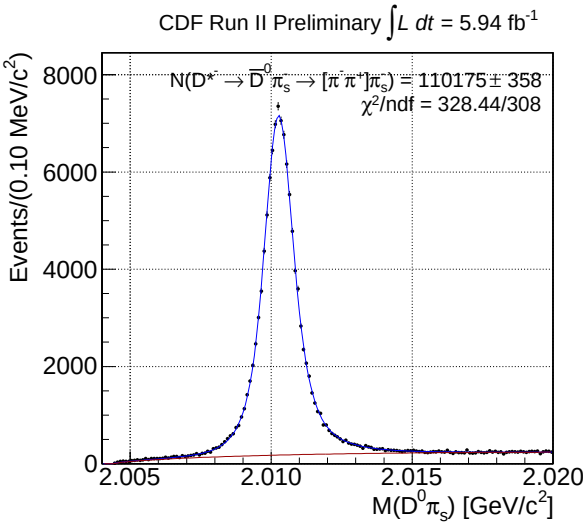

(b)

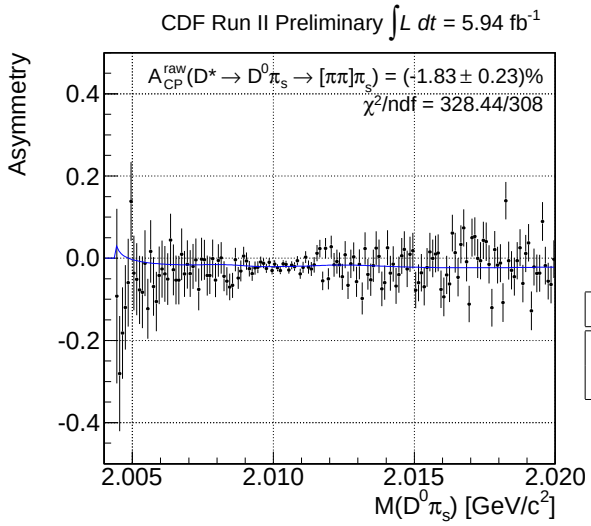

(c)

(d)

PAR	POS VALUE	NEG VALUE	ASYMMETRY
$N_{\rm sgn}$	106216 ± 352	110175 ± 358	$(-1.83 \pm 0.23)\%$
$N_{\rm bkg}$	26554 ± 209	27928 ± 213	$(-2.52 \pm 0.55)\%$